REMARKS

Favorable consideration of this application is respectfully requested in view of the foregoing amendment and the following remarks. Claims 1-5, 7-15, 18 and 19 are pending in the application. Claim 1 has been amended to incorporate the features recited in claims 18-19. Accordingly, claims 18-19 have been cancelled without prejudice. New claim 20 has been added and depends from claim 9. Support for claim 20 is found in originally filed claim 9 and throughout the specification. Applicant respectfully requests entry of the amendment.

Claims 1, 4, 7, 8 and 9 have been rejected under 35 U.S.C. §102(a) as being anticipated by Dimitroff. In particular, the Examiner states:

> "Dimitroff et al. discloses a method for treating neovasculature in a subject comprising administering an effective amount of an anti-angiogenic agent to the subject, administering an effective amount of a photosensitive agent to the subject, and irradiating the neovasculature with light having a wavelength absorbable by the photosensitive agent."

The Examiner further states on page 6 (Response to Arguments) with respect to Dimitroff et al. that

> "Applicant argues that Dimitroff et al. fails to indicate ocular neovascularization. Examiner respectfully disagrees. Specifically, on page 122, second column, second paragraph, there is disclosure of experimental models of iris and retinal angiogenesis."

Applicant respectfully disagrees with the Examiner's assertions and conclusion and submits that claims 1, 4, 7, 8 and 9 are not anticipated by Dimitroff et al. for the reasons stated below.

Dimitroff et al. teach that a combination treatment involving photodynamic therapy (PDT) followed by therapy with the tyrosine kinase inhibitors, PD166285 and PD173074, was effective in suppressing and delaying tumor regrowth. While Dimitroff et al. indicate that PD173074 demonstrated anti-angiogenic effects on fibroblast growth factor-induced corneal neovascularization (see introduction section page 122), Dimitroff et al. fail to teach that a combination treatment of PDT and PD166285 or PD173074 would be effective in treating unwanted ocular neovascularization in a subject suffering from choroidal or retinal neovascularization as recited in amended independent claim 1.

With respect to the Examiner's statement that "Applicant argues that Dimitroff fails to indicate ocular neovascularization" (see page 6 of the outstanding Office Action), Applicant asserts that this is not an accurate characterization of what Applicant actually stated in the previous Amendment dated August 4, 2004. Applicant actually stated in the previous Amendment (see page 4, last paragraph) that "Dimitroff et al., however, fail to indicate that such a therapeutic combination [i.e., PD166285 or PD173074 combined with PDT] is useful to treat unwanted ocular neovascularization."

With respect to the Examiner's contention that Dimitroff et al. on page 122, second column, second paragraph, indicate ocular neovascularization in its disclosure of experimental models of iris and retinal angiogenesis, it is noted that the referenced articles in Dimitroff et al. (see Dimitroff et al., references 23 and 24, Wilson et al., Ophthal. & Vis. Sci., Vol. 32(9):2530-5, 1991 and Miller et al. Ophthalmology, Vol. 98(11):1711-9, 1991, respectively; copies of which are attached) pertaining to the disclosure of experimental models of iris and retinal angiogenesis do not describe experimental models of iris and retinal angiogenesis utilizing a combination therapy of PDT and PD166285 or PD173074. Instead, the referenced articles (ref. 23 an 24) in Dimitroff et al. describe experimental models of iris and retinal angiogenesis utilizing treatment with PDT alone. Accordingly, since Dimitroff et al. does not specifically teach the use of a combination of PDT and PD166285 or PD173074 to treat unwanted ocular neovascularization in a subject suffering from retinal or choroidal neovascularization, Dimitroff et al. does not anticipate amended independent claim 1.

In view of the above, withdrawal of the rejection of claims 1, 4, 7, 8 and 9 under 35 U.S.C §102(a) is respectfully requested.

Claims 9 and 10 have been rejected under 35 U.S.C. §102(e) as being anticipated by U.S. Patent 6,214,819 (Brazzell et al. '819). In particular, the Examiner states "Brazzell et al. ('819) discloses wherein the anti-angiogenic agent is N-benzoyl-staurosporine." Applicant respectfully disagrees with the Examiner's assertion and conclusion and submits that Brazzell et al. '819 do not anticipate claims 9 and 10.

Brazzell et al. '819 describe a method of treating ocular neovascularization by administering a staurosporine derivative. Brazzell et al. '819, however, do not describe that a combination treatment of staurosporine and PDT therapy would be effective in treating unwanted ocular neovasculature in a subject suffering from choroidal or retinal neovascularization as recited in claims 9 and 10, which depend from amended claim 1. Since Brazzell et al. '819 do not identically describe claims 9 and 10, Brazzell et al. '819 do not anticipate claims 9 and 10.

In view of the above, withdrawal of the rejection of claims 9 and 10 under 35 U.S.C. §102(e) is respectfully requested.

Claims 1, 3, 18 and 19 have been rejected under 35 U.S.C. §103(a) as being unpatentable over U.S. Patent 6,297,228 (Clark) in view of Dimitroff et al.

Clark describes treating ocular neovascular diseases utilizing a combination of PDT and angiostatic steroids such as anacortave acetate. Dimitroff et al. describe utilizing the tyrosine kinase inhibitors, PD166285 and PD173074, in combination with PDT to inhibit tumor growth. Dimitroff et al., however, do not teach or specifically suggest that PD166285 and PD173074 can be used in combination with PDT to treat ocular neovascularization in a subject suffering from choroidal or retinal neovascularization. In addition, neither Dimitroff et al. nor Clark indicate that PD166285 and PD173074 can be substituted for the steroid, anecortave acetate, and combined

with PDT to treat ocular neovascularization in a subject suffering from choroidal or retinal vascularization. Further, it is not apparent where Dimitroff et al. disclose antagonists of growth hormone, antagonists of IGF-1, inhibitors of cyclooxygenase II, antagonists of angiotensin II, antagonists of NF-kappa B and phopholipase A2 antagonists as asserted by the Examiner on page 4 of the outstanding Action. Applicant requests that the Examiner indicate on which page and column such antagonists/inhibitors are described in Dimitroff et al.

In view of the above, it is Applicant's position that the combination of Clark and Dimitroff et al. does not make obvious amended independent claim 1. Accordingly, withdrawal of the rejection of claims 1, 3, 18 and 19 under 35 U.S.C. §103(a) is respectfully requested.

Claims 2, 4, 5 and 13-15 have been rejected under 35 U.S.C. §103(a) as being unpatentable over Clark in view of Dimitroff et al.

With respect to this §103 rejection, the same arguments proffered above to address the §103 rejection of claims 1, 3, 18 and 19 are applicable to the §103 rejection of claims 2, 4, 5 and 13-15, namely that Dimitroff et al. do not teach or specifically suggest that PD166285 and PD173074 can be used in combination with PDT to treat ocular neovascularization in a subject suffering from retinal or choroidal vascularization Further, neither Dimitroff et al. nor Clark indicate that PD166285 and PD173074 can be substituted for anecortave acetate and combined with PDT to treat ocular neovascularization in a subject suffering from retinal or choroidal vascularization. Accordingly, the combination of Clark and Dimitroff et al. does not make obvious claims 2, 4, 5 and 13-15.

In view of the above, withdrawal of the rejection of claims 2, 4, 5 and 13-15 under 35 U.S.C. §103(a) is respectfully requested.

Claims 11 and 12 have been rejected under 35 U.S.C. §103(a) as being unpatentable over Clark in view of Dimitroff et al. and further in view of U.S. Patent 5,770,619 (Richter et al.).

With respect to this §103 rejection, the same arguments proffered above to address the §103 rejections of claims 1, 3, 18 and 19 and claims 2, 4, 5 and 13-15 are applicable to the §103 rejection of claims 11 and 12, namely that Dimitroff et al. do not teach or specifically suggest that PD166285 and PD173074 can be used in combination with PDT to treat ocular neovascularization in a subject suffering from retinal or choroidal neovascularization. Further, neither Dimitroff et al. nor Clark teach or specifically suggest that PD166285 and PD173074 can be substituted for anecortave acetate and combined with PDT to treat ocular neovascularization. Richter et al. in disclosing that photosensitive agents can be selected from the group consisting of a porphyrin, a purpurin and a benzoporphyrin derivative monoacid ring A do not remedy the deficiencies present in Clark and Dimitroff et al. Accordingly, the combination of Clark, Dimitroff et al. and Richter et al. does not make obvious claims 11 and 12.

In view of the above, withdrawal of the rejection of claims 11 and 12 under 35 U.S.C. §103(a) is respectfully requested.

Claims 11 and 12 have been rejected under 35 U.S.C. §103(a) as being unpatentable over Dimitroff et al., in view of Richter et al.

While Dimitroff et al. teach that PD166285 and PD173074 can be combined with PDT to suppress or delay tumor growth, Dimitroff et al. fail to teach that such a combination treatment could be utilized to treat unwanted ocular neovascularization in a subject suffering from choroidal or retinal neovascularization. Richter et al. in disclosing that photosensitive agents can be selected from the group consisting of a porphyrin, a purpurin and a benzoporphyrin derivative monoacid ring A do not remedy the deficiencies present in Dimitroff et al. Accordingly, the combination of Dimitroff et al. and Richter et al. does not make obvious claims 11 and 12.

In view of the above, withdrawal of the rejection of claims 11 and 12 under 35 U.S.C. §103(a) is respectfully requested.

A good faith effort has been made to place the present application in condition for allowance. If the Examiner believes a telephone conference would be of value, she is requested to call the undersigned at the number listed below.

Respectfully submitted

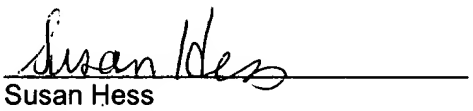

Novartis
Corporate Intellectual Property
One Health Plaza, Building 104
East Hanover, NJ 07936-1080
(862) 778-7859

Susan Hess
Attorney for Applicant
Reg. No. 37,350

Date: June 2, 2005

Investigative Ophthalmology & Visual Science. Vol. 32, No. 9, August 1991

Treatment of Experimental Preretinal Neovascularization Using Photodynamic Thrombosis

Charles A. Wilson,* Peter Saloupis,* and Diane L. Hatchell*†‡

Retinal or preretinal neovascularization (NV) is the result of many ischemic conditions of the retina and is an important factor leading to severe visual loss in diabetic retinopathy. Panretinal photocoagulation does not always control its growth or bleeding sequelae. A potential new treatment modality, photodynamic therapy (PDT), was evaluated for limiting the progression of experimental NV in the rabbit eye. The NV was produced by injecting cultured dermal fibroblasts into the preretinal vitreous space after combined enzymatic and mechanical vitreolysis. This method results in traction retinal detachment with a rapid and consistent growth of NV. After administration of the photosensitizing dye rose bengal (20 mg/kg intravenously), PDT was done using a slit-lamp light source focused through a fundus contact lens (45 J/cm²). The NV was treated on two separate occasions during the active phase of growth (on days 13 and 21 after fibroblast injection). Control animals were exposed to light before injection of rose bengal. Eight randomly assigned animals in each group were followed between treatments and for 28 days after the second treatment. The appearance of NV was documented by frequent photography and fluorescein angiography. The PDT resulted in thrombosis of NV for at least 3 days. Reperfusion, however, was consistently noted at 7 days. Thrombosis was associated with a delay in the growth and maturation of NV fronds, which resumed after reperfusion. Twenty-eight days after the second treatment, NV in both experimental and control eyes had undergone atrophy. At that time (the conclusion of follow-up), however, the size of treated NV fronds (estimated from computerized image analysis of fluorescein angiograms) was significantly less than that of controls. Thus, PDT offers promise as an adjunctive means of temporarily obliterating or stemming the growth of NV in the proliferative retinopathies. Invest Ophthalmol Vis Sci 32:2530–2535, 1991

Preretinal neovascularization (NV) is a manifestation of diabetic retinopathy and many other diseases. Untreated NV may progress to severe visual loss due to vitreous hemorrhage or, more significantly, retinal detachment. Panretinal photocoagulation usually produces regression of NV, for reasons which are uncertain. The practice of focally treating new vessels to occlude them, although advocated during the development of photocoagulation treatment, generally requires light energies which also produce extensive, full-thickness retinal damage.[1] Therefore, focal treatment of NV has been replaced largely by scatter photocoagulation techniques that require less energy and produce less thermal effects on inner retinal layers. Despite recommended amounts of laser treatment, however, progression of NV has been observed in some individuals.[2] We wished to develop an alternative treatment for NV that avoids the thermal effects of laser photocoagulation and, therefore, evaluated a potential new modality, photodynamic therapy (PDT), in an animal model of preretinal NV.

In PDT, a photosensitizing dye is administered systemically and activated in blood vessels or other tissues by light of a suitable wavelength. Biologically reactive molecules are produced which lead to tissue damage or, in the case of blood vessels, thrombosis. Most importantly, the photobiologic effects can be produced without substantially heating tissues.[3] Potential ophthalmologic uses of PDT that have been explored in animal models include the treatment of corneal[4–6] and iris[7] NV and uveal tumors.[3,8–10] One photosensitizing agent, hematoporphyrin derivative, has been used in humans for the treatment of choroidal melanoma preliminarily.[11]

Our study examined the effect of PDT on actively growing NV tufts in a recently developed rabbit model of vitreoretinal fibroblast proliferation.[12] The model was chosen because of its rapid and consistent production of NV tufts over the optic disc and medul-

From the *Department of Ophthalmology, the †Department of Cell Biology, Duke University Medical Center, and the ‡Durham Veterans Administration Medical Center, Durham, North Carolina.

Supported by Veterans Administration medical research funds and National Institutes of Health research grant EY02903 and core grant EY05722. Dr. Hatchell is a Research to Prevent Blindness, Inc. Senior Scientific Investigator.

Submitted for publication: February 9, 1991; accepted April 12, 1991.

Reprint requests: Diane L. Hatchell, PhD, Department of Ophthalmology, Duke University Medical Center, Box 3802, Durham, NC 27710.

lary rays. Rose bengal, previously shown to be effective in producing photochemical thrombosis of normal retinal vessels in the rabbit eye,[13,14] was used as the photosensitizer.

Materials and Methods

Animals

These experiments were done in accordance with the ARVO Resolution on the Use of Animals in Research. The 16 Dutch-belted rabbits (weight range, 1.0–1.9 kg) used in this study were divided randomly into two equal groups (treatment and control) on day 12 after fibroblast implantation (vide infra), at which time the presence of NV could be documented clinically.

Before treatment or examination, the rabbits were anesthetized with ketamine HCl (25–50 mg/kg intramuscularly) and xylazine HCl (5–10 mg/kg intramuscularly). For treatment, the pupils were dilated using cyclopentolate 1% and phenylephrine 2.5%. Pupillary dilation was maintained between follow-up examinations with atropine 1% ointment, which was applied after each examination or treatment.

Production of Preretinal NV

The method developed by Antoszyk et al[12] was used because it produces a high yield of NV. In their study, 95% of eyes developed clinically evident NV by day 14 after intravitreal injection of homologous dermal fibroblasts. Briefly, the method consists of repeated preretinal injection and aspiration of 1 IU of hyaluronidase (in 0.1 ml phosphate-buffered saline [PBS]) over the optic disc and medullary rays. Studies in normal rabbit eyes showed that this dose of hyaluronidase was well tolerated by the retina.[15] Vitreolysis was assisted by sweeping a 25-gauge needle over the medullary rays. Residual hyaluronidase solution and vitreous was aspirated eventually (0.2 ml). Homologous dermal fibroblasts, harvested and cultured as described previously,[12] were injected into the area of vitreolysis (2.5×10^5 cells/0.1 ml PBS) and allowed to disperse in the area of the medullary rays.

PDT

The PDT was done by first positioning the animal on a adjustable stage mounted on a Topcon photo slit lamp (model SL-5D; Paramus, NJ) and stabilizing its head in a stereotactic device. The light intensity of the slit lamp was set to high, and the heat-absorbing filter resident on the instrument was positioned. This filter's transmission is less than 12% at wavelengths greater than 900 nm. The resulting irradiance, measured with a YSI-Kettering model 65A radiometer (Yellow Springs Instrument, Yellow Springs, OH), was 73 mW/cm^2. A circular spot of light, 2–5 mm in diameter (slit-lamp setting), was centered and focused on the NV through a plano fundus contact lens, taking care to avoid direct light exposure of the iris. The smallest spot diameter was selected that covered the entire visible area of NV.

Rose bengal (certified purity 90%; Sigma, St. Louis, MO) was prepared in a concentration of 20 mg/ml in normal saline and sterilized by aspiration through a 0.22-μm filter. With the animal in position as described, the dye was injected (20 mg/kg) through a marginal ear vein. Light exposure was continued for another 10 min (45 J/cm^2), after which the rabbit was transferred to a dimly lit room and allowed to recover. Treatments were done during the active phase of NV proliferation: 13 days after fibroblast injection and 8 days later. Control animals underwent the same procedure, except that the rose bengal was injected after the light exposure was completed.

Clinical Examinations

Follow-up examinations consisted of indirect ophthalmoscopy, color fundus photography, and fluorescein angiography at baseline (1 day before the first treatment [12 days after fibroblast injection]); 1, 3, and 7 days after the first treatment; and 1, 3, 7, 14, and 28 days after the second treatment. In the model, NV undergoes spontaneous involution within 42 days.[12] Accordingly, an observation period of 49 days was allowed.

Image Analysis

The size of the NV tufts was estimated by measuring the area of perfused NV in all fluorescein angiograms. To avoid inaccuracies from fluorescein leakage and spread, early-phase photographs were studied. Image analysis was facilitated by the focal nature of NV in the model. One control eye, however, was excluded from analysis because its NV was multicentric and could not be photographed adequately.

Photographic negatives were placed on a light box and viewed by a video camera through a Zeiss dissecting microscope (Carl Zeiss, Inc., Thornwood, NY). Images were digitized and captured on a video board mounted in a International Business Machines 386 microcomputer (Boca Raton, FL) operating JAVA software (Jandel, Corte Madera, CA). The system was calibrated using a standardized area (a notch) found at one corner of each photographic field. This area was defined as 100 square units. The NV was measured by outlining the fluorescein-filling area with the mouse-directed cursor. The area in the outline was computed using the software.

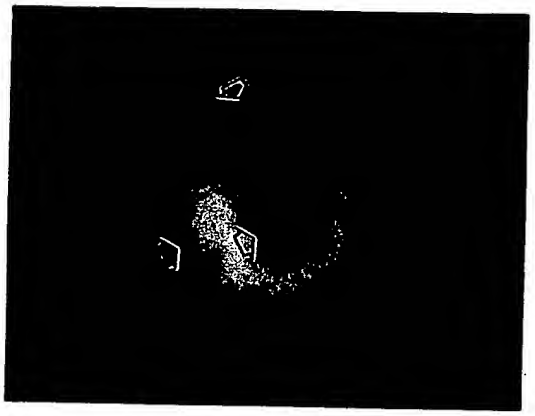

Fig. 1. Fundus photograph showing the slit-lamp biomicroscopic appearance of neovascularization during photodynamic treatment. The illuminated area (solid arrow) includes the neovascular tuft (open arrows). Detached retina surrounds the tuft.

Results

The PDT resulted in a change in the color of the NV tuft from bright to dark red during the 10-min course of light exposure (Fig. 1). Near the end of the treatment, stagnant blood (as evidenced by interruptions in the continuity of the red cell column) occasionally could be visualized in some vessels. When normal myelin wing vessels were in the field of illumination, they underwent partial or complete thrombosis during the course of treatment. Control eyes showed no clinically apparent changes during light exposure.

After treatment, fluorescein angiography revealed nonperfusion of preretinal NV (Fig. 2). Total nonperfusion was seen on posttreatment day 1, with NV silhouetted against the background of choroidal fluorescence. By posttreatment day 3, however, some eyes showed small areas of fluorescein filling and leakage,

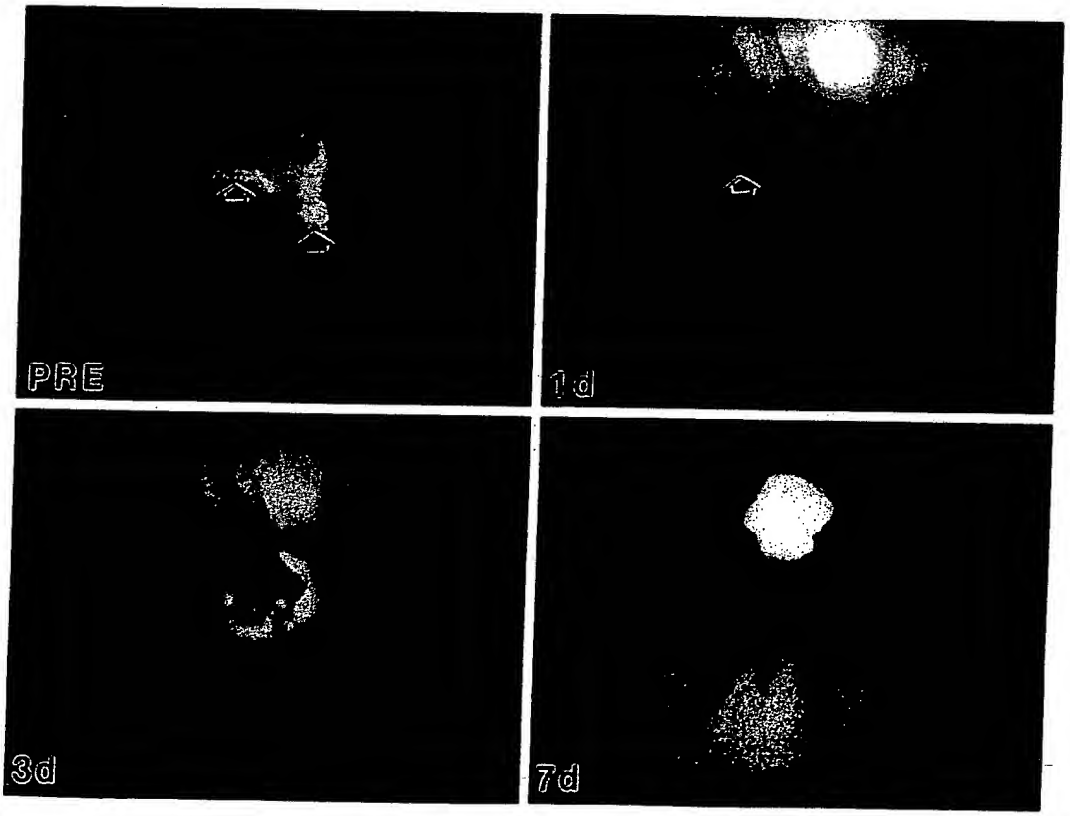

Fig. 2. Angiographic appearance of neovascularization pre- and 1, 3, and 7 days after the first photodynamic treatment. Before treatment, early neovascular growth is noted (solid arrow) adjacent to normal medullary ray vessels (open arrow). Total nonperfusion of both new and normal (open arrow) vessels is observed on post-treatment day 1. At day 3, fluorescein leakage appears behind the neovascular tuft. Finally, at day 7, the neovascularization appears completely reperfused.

usually at the
eyes showed
The second tr
orrhagic con
time. Control
of nonperfusi

The PDT s
of NV (estin
computerized
trols at most
each treatme
7 days, man
area. Betwee
ment, there
increase in N
with the trea
The differen
< 0.05) at bc
and at all e>
(Figs. 3, 4).

The clinic
inal NV was
inal fibrobla
apart, each p
perfusion ge
posttreatmer
delayed by t

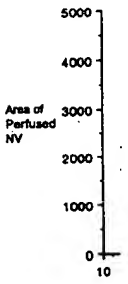

Fig. 3. Area
intravitreal fib
circles) showed
cularization (c
days 13 and 2
day 3 after th
treated eyes w
two-tailed) of
lows: 12 days
20 days ($P = 0.$
($P < 0.001$),
represent the

usually at the base of the NV tuft. At day 7, NV in all eyes showed complete or near-complete reperfusion. The second treatment reproduced these events. Hemorrhagic complications were not observed at any time. Control eyes showed no angiographic evidence of nonperfusion after light treatment.

The PDT significantly decreased the perfused area of NV (estimated from fluorescein angiograms by computerized image analysis) compared with controls at most follow-up examinations (Fig. 3). After each treatment, there was a reperfusion of NV within 7 days, manifested as a rapid increase in perfused area. Between 7 and 28 days after the second treatment, there appeared to be a slower, parallel rate of increase in NV area in the treated and control groups, with the treated NV consistently remaining smaller. The difference between groups was significant ($P < 0.05$) at both 1 and 3 days after the first treatment and at all examinations after the second treatment (Figs. 3, 4).

Discussion

The clinical effects of PDT on the growth of preretinal NV was examined in a rabbit model of vitreoretinal fibroblast proliferation. Two treatments, 8 days apart, each produced temporary occlusion of NV. Reperfusion generally occurred between 3 and 7 days posttreatment. Growth and maturation of NV was delayed by treatment but not prevented. Treated NV continued to enlarge after reperfusion, but they were smaller than control NV.

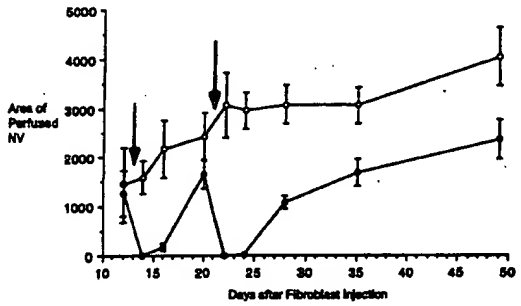

Fig. 3. Area of perfused neovascularization versus days following intravitreal fibroblast injection. Control neovascularization (open circles) showed progressive increase in area, whereas treated neovascularization (closed circles) was temporarily occluded by PDT on days 13 and 21 (arrows). All means represent eight eyes, except at day 3 after the second treatment, when five control and three treated eyes were measured. Statistical comparisons (student t-test, two-tailed) of groups at each follow-up examination were as follows: 12 days ($P = 0.75$), 14 days ($P < 0.001$), 16 days ($P = 0.003$), 20 days ($P = 0.19$), 22 days ($P < 0.001$), 24 days ($P < 0.001$), 28 days ($P < 0.001$), 35 days ($P = 0.01$), 49 days ($P = 0.03$). Variances represent the SEM.

The duration of NV occlusion in this study was similar to photodynamic occlusions produced in normal rabbit medullary ray vessels.[13,14] In these studies, reperfusion occurred by 3 days in major arterioles and by 7 days in major venules. Other reports were mixed regarding the duration of photodynamic vascular occlusion. In the cat eye, rose bengal-sensitized damage of the retinal microvasculature and choriocapillaris produced extensive areas of occlusion with relatively little reperfusion after 4 months of follow-up.[16] Although the major retinal vessels remained perfused, they were not directly targeted during treatment. In a rabbit model of corneal NV, PDT using rose bengal produced long-lasting vessel occlusion.[6] The mechanism of vessel injury, however, was unclear since argon laser irradiation (514.5 nm) was used at a sufficient power to generate a combined thermal–photochemical reaction. Another photosensitizing agent, hematoporphyrin derivative, was used to obliterate iris NV in a primate model of branch retinal vein occlusion.[7] Two of four treated eyes were followed longer than 1 day. Of these, one eye had recurrent (or reperfused) iris NV 8 days after the initial treatment. A second treatment abolished iris leakage for the duration of follow-up (2 months).

There are several factors that may influence the duration of vascular occlusion after PDT. Among these are the composition and size of the clot. Previous studies showed that the initial event leading to vascular thrombosis in PDT is endothelial cell injury and platelet adherence.[17] The resulting clot is fibrin poor, and consequently it is believed to resist the effects of degradation initiated by tissue plasminogen activator.[6,18] However, fibrin polymer stabilizes platelet plugs, and its scarcity could result in a less stable occlusion. In addition, relatively small clots may not occlude vessels completely or could become fragmented by hemodynamic forces. Another factor that could influence the duration of vascular occlusion is the rate of endothelial cell repair or regeneration. In actively growing NV, a number of retinal endothelial cells are already in a proliferative state. Provided that the initial stimulus for proliferation remains after PDT, uninjured endothelial cells could repopulate damaged vessel lumina or form additional new vessels rapidly. Because mature NV fronds were not evaluated in our study, their response to PDT is uncertain.

The NV growth was estimated by computerized image analysis of fluorescein angiograms. This technique has several obvious disadvantages. First, it is only capable of detecting NV growth in two dimensions; and second, it is subject to error related to ante-

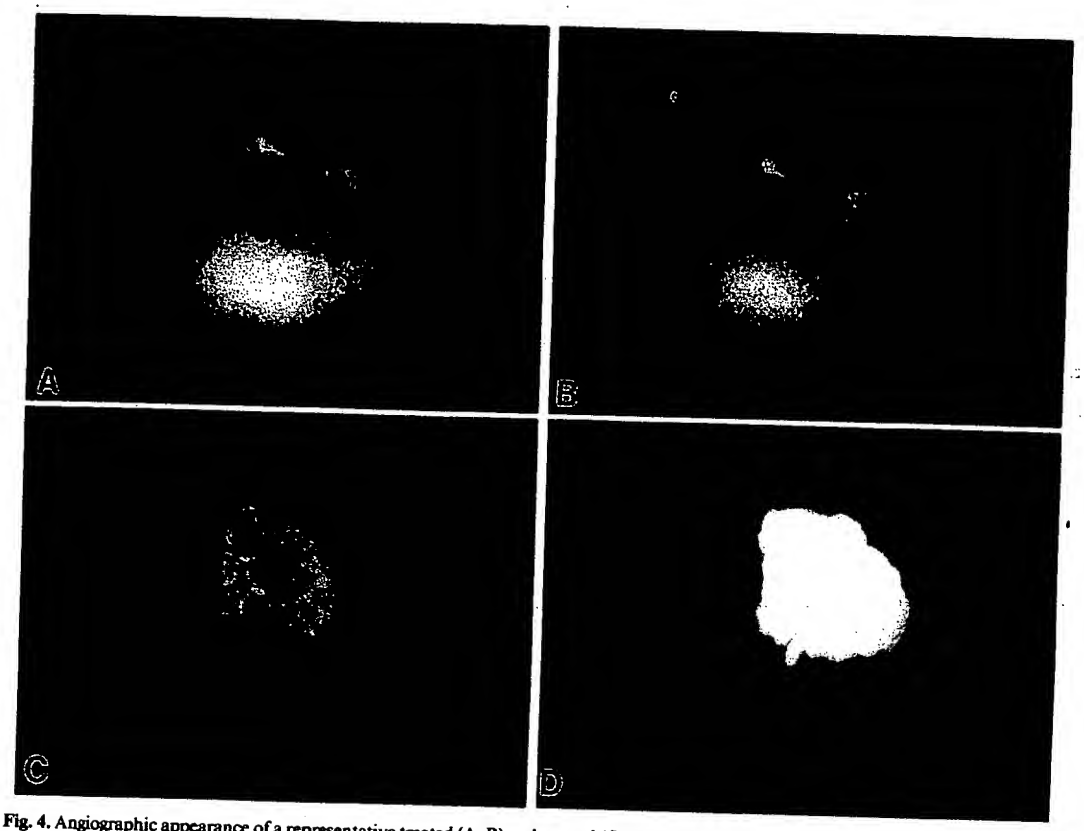

Fig. 4. Angiographic appearance of a representative treated (A, B) and control (C, D) neovascularization 28 days after the second treatment. Early phases are shown in (A) and (C); late phases are shown in (B) and (D). The control neovascularization is slightly larger and shows greater fluorescein leakage than the treated frond.

rior displacement of NV from the fundus which produces a change in image magnification. Fortunately, magnification changes would tend to reduce rather than increase the observed difference between large and small NV tufts. This is because large, extensive NV fronds generally were highly elevated, frequently growing onto and along the posterior lens surface. Small tufts, by virtue of a more posterior location, were relatively magnified. Despite these limitations, image analysis provided an objective estimation of NV growth in vivo that would not have been possible otherwise.

There are several mechanisms by which PDT could limit the growth of NV. Most directly, thrombosis of parent vessels deprives potential newer vessel buds of blood supply. Decreased blood supply could also "starve" surrounding tissues including fibroblast colonies. In this case, fibroblasts and perhaps other host cells might either stop proliferating or die, thus interrupting the process of vitreoretinal fibroplasia. Fibroblasts produce a collagen matrix that could be important for the development of NV. A prominent, multilayered extracellular matrix has been associated with developing NV in a similar rabbit model.[19] Collagen is also one striking feature of many preretinal fibrovascular membranes in severe proliferative diabetic retinopathy.[20]

The cause of NV in this rabbit model is uncertain. Therefore, its relevance to the proliferative retinopathies in humans must be viewed with uncertainty. However, the model does provide a reproducible form of NV that is localized conveniently and documented and treated easily. The development of NV was described in the rabbit eye using methylmethacrylate vascular casts.[21] The new vessels budded from retinal veins as early as 3 days after autotransplantation of dermal fibroblasts. They grew into a fibrous tissue matrix and, as early as 4 weeks, formed distal tortuosities and glomerular-like structures. After 3 months, there was an apparent reduction in the overall number of new vessels. In a more recent study, the ultrastructural features of rabbit NV were examined

at various stages of development and were found to resemble those seen in retinopathy of prematurity and proliferative diabetic retinopathy.[19]

Effective treatments were developed that lower the risk of complications from proliferative retinopathy. In proliferative diabetic retinopathy, laser panretinal photocoagulation generally is indicated, but sometimes it does not prevent progressive NV.[2] Therefore PDT potentially is useful in these instances as an adjunctive treatment. One drawback of this approach is that PDT damages normal vessels and NV. It therefore might be better suited for treating peripheral NV than proliferations in the posterior pole. Other photosensitizing agents have been identified (ie, hematoporphyrin derivative and phthalocyanine dyes[3]) that may be selectively retained in certain tissues, particularly in vascularized tumors. These agents also could be evaluated to determine if photothrombosis can be produced more selectively in NV. Another drawback of PDT is that occlusion of NV is not permanent, even after a second treatment. Perhaps, a combination of low-intensity laser (thermal) and photochemical damage would extend the duration of vascular closure. We currently are exploring these possibilities.

In summary, dye-sensitized photothrombosis of preretinal NV was evaluated in a rabbit model. Two treatments, separated by an interval of 8 days, each completely occluded visible areas of NV. Reperfusion occurred generally from days 3–7. The growth of NV was delayed by treatment, and the size of the NV tuft during the follow-up period was less than that of controls.

Key words: photodynamic therapy, rose bengal, retina, neovascularization, singlet oxygen

Acknowledgments

The authors thank James S. Tiedeman, MD, PhD, for his assistance in the preparation of this manuscript.

References

1. Davis MD: Proliferative diabetic retinopathy. *In* Retina, Ryan SJ, editor. St. Louis, CV Mosby, 1989, pp. 367–402.
2. Vine AK: The efficacy of additional argon laser photocoagulation for persistent, severe proliferative diabetic retinopathy. Ophthalmology 92:1532, 1985.
3. Panagopoulos JA, Svitra PP, Puliafito CA, and Gragoudas ES: Photodynamic therapy for experimental intraocular melanoma using chloroaluminum sulfonated phthalocyanine. Arch Ophthalmol 107:886, 1989.
4. Mendelsohn AD, Watson BD, Alfonso EC, Lieb M, Mendelsohn GP, Forster RK, and Dennis JJ: Amelioration of experimental lipid keratopathy by photochemically induced thrombosis of feeder vessels. Arch Ophthalmol 105:983, 1987.
5. Huang AJW, Watson BD, Hernandez E, and Tseng SCG: Photothrombosis of corneal neovascularization by intravenous rose bengal and argon laser irradiation. Arch Ophthalmol 106:680, 1988.
6. Correnl G, Roussel TJ, Tseng SCG, and Watson BD: Promotion of graft survival by photothrombotic occlusion of corneal neovascularization. Arch Ophthalmol 107:1501, 1989.
7. Packer AJ, Tse DT, Gu X-Q, and Hayreh SS: Hematoporphyrin photoradiation therapy for iris neovascularization. Arch Ophthalmol 102:1193, 1984.
8. Gomer CJ, Doiron DR, White L, Jester JV, Dunn S, Szirth BC, Razum NJ, and Murphree AL: Hematoporphyrin derivative photoradiation induced damage to normal and tumor tissue of the pigmented rabbit eye. Curr Eye Res 3:229, 1984.
9. Sery TW and Dougherty TJ: Photoradiation of rabbit ocular malignant melanoma with hematoporphyrin derivative. Curr Eye Res 3:519, 1984.
10. Winward KE, Dabbs CK, Olsen K, Watson BD, Hernandez E, and DiBernardo C: Encircling photothrombotic therapy for choroidal Greene melanoma using rose bengal. Arch Ophthalmol 108:588, 1990.
11. Tse DT, Dutton JJ, Weingeist TA, Hermsen VM, and Kersten RC: Hematoporphyrin photoradiation therapy for intraocular and orbital malignant melanoma. Arch Ophthalmol 102:833, 1984.
12. Antoszyk AN, Gottlieb JL, Casey R, Hatchell DL, and Machemer R: An experimental model of preretinal neovascularization in the rabbit. Invest Ophthalmol Vis Sci 32:46, 1991.
13. Nanda SK, Hatchell DL, Tiedeman JS, Dutton JJ, Hatchell MC, and McAdoo T: A new method for vascular occlusion: Photochemical initiation of thrombosis. Arch Ophthalmol 105:1121, 1987.
14. Royster AJ, Nanda SK, Hatchell DL, Tiedeman JS, Dutton JJ, and Hatchell MC: Photochemical initiation of thrombosis: Fluorescein angiographic, histologic, and ultrastructural alterations in the choroid, retinal pigment epithelium, and retina. Arch Ophthalmol 106:1608, 1988.
15. Gottlieb JL, Antoszyk AN, Hatchell DL, and Saloupis P: The safety of intravitreal hyaluronidase: A clinical and histologic study. Invest Ophthalmol Vis Sci 31:2345, 1990.
16. Wilson CA, Royster AJ, Tiedeman JS, and Hatchell DL: Exudative retinal detachment following photodynamic injury. Arch Ophthalmol 109:125, 1991.
17. Povlishock JT, Rosenblum WI, Sholley MM, and Wei ED: An ultrastructural analysis of endothelial change paralleling platelet aggregation in a light/dye model of microvascular insult. Am J Pathol 110:148, 1983.
18. Watson BD, Dietrich WD, Prado R, and Ginsberg MD: Argon laser-induced arterial photothrombosis: Characterization and possible application to therapy of arteriovenous malformations. J Neurosurg 66:748, 1987.
19. deJuan E Jr, Humayun MS, Hatchell DL, and Wilson D: Histopathology of experimental preretinal neovascularization. Invest Ophthalmol Vis Sci 30:1495, 1989.
20. Hamilton CW, Chandler D, Klintworth GK, and Machemer R: A transmission and scanning electron microscopic study of surgically excised preretinal membrane proliferations in diabetes mellitus. Am J Ophthalmol 94:473, 1982.
21. Tano Y, Chandler DB, and Machemer R: Vascular casts of experimental retinal neovascularization. Am J Ophthalmol 92:110, 1981.

Investigational New Drugs 17: 121–135, 1999.

Anti-angiogenic activity of selected receptor tyrosine kinase inhibitors, PD166285 and PD173074: Implications for combination treatment with photodynamic therapy

Charles J. Dimitroff[1], Wayne Klohs[2], Amarnath Sharma[3], Paula Pera[1], Denise Driscoll[2], Jean Veith[1], Randall Steinkampf[2], Mel Schroeder[2], Sylvester Klutchko[2], Adam Sumlin[5], Barbara Henderson[5], Thomas J. Dougherty[4] and Ralph J. Bernacki[4]

[1]*Harvard Skin Disease Research Center, Harvard Medical School, Boston, MA;* [2]*Parke-Davis Pharm. Research, Division of Warner-Lambert, Ann Arbor, MI;* [3]*SmithKline Beecham Pharmaceutical, Department of Drug Metabolism and Pharmacokinetics, King of Prussia, PA;* [4]*Roswell Park Cancer Institute, Grace Cancer Drug Center, Department of Pharmacology and Therapeutics;* [5]*Department of Photodynamic Therapy, Buffalo, NY, USA*

Key words: angiogenesis, cytostatic chemotherapy, tyrosine kinase inhibitors

Summary

Angiogenesis, the formation of new blood vessels from an existing vasculature, is requisite for tumor growth. It entails intercellular coordination of endothelial and tumor cells through angiogenic growth factor signaling. Interruption of these events has implications in the suppression of tumor growth. PD166285, a broad-spectrum receptor tyrosine kinase (RTK) inhibitor, and PD173074, a selective $FGFR_1TK$ inhibitor, were evaluated for their anti-angiogenic activity and anti-tumor efficacy in combination with photodynamic therapy (PDT). To evaluate the anti-angiogenic and anti-tumor activities of these compounds, RTK assays, *in vitro* tumor cell growth and microcapillary formation assays, *in vivo* murine angiogenesis and anti-tumor efficacy studies utilizing RTK inhibitors in combination with photodynamic therapy were performed. PD166285 inhibited PDGFR-ß-, EGFR-, and $FGFR_1TKs$ and c-src TK by 50% (IC_{50}) at concentrations between 7–85nM. PD173074 displayed selective inhibitory activity towards $FGFR_1TK$ at 26nM. PD173074 demonstrated (>100 fold) selective growth inhibitory action towards human umbilical vein endothelial cells compared with a panel of tumor cell lines. Both PD166285 and PD173074 (at 10nM) inhibited the formation of microcapillaries on Matrigel-coated plastic. *In vivo* anti-angiogenesis studies in mice revealed that oral administration (p.o.) of either PD166285 (1–25 mg/kg) or PD173074 (25–100 mg/kg) generated dose dependent inhibition of angiogenesis. Against a murine mammary 16c tumor, significantly prolonged tumor regressions were achieved with daily p.o. doses of PD166285 (5–10 mg/kg) or PD173074 (30–60 mg/kg) following PDT compared with PDT alone ($p<0.001$). Many long-term survivors were also noted in combination treatment groups. PD166285 and PD173074 displayed potent anti-angiogenic and anti-tumor activity and prolonged the duration of anti-tumor response to PDT. Interference in membrane signal transduction by inhibitors of specific RTKs (e.g. $FGFR_1TK$) should result in new chemotherapeutic agents having the ability to limit tumor angiogenesis and regrowth following cytoreductive treatments such as PDT.

Introduction

Platelet-derived growth factor (PDGF), basic fibroblast growth factor (bFGF), epidermal growth factor (EGF) and vascular endothelial growth factor (VEGF) represent potent, endogenous mitogens of physiologic angiogenesis. Their receptors contain a cytoplasmic tyrosine kinase that initiates signaling pathways affecting endothelial cell proliferation and differentiation [1,2]. The roles of these growth factors in coordinating blood vessel development are not clearly understood, but recent reports suggest that these

growth factors regulate, although differentially, *de novo* synthesis of blood vessels, vascular remodeling and tumor angiogenesis [3–5]. These factors stimulate angiogenic phenomena characterized by the proliferation, migration and invasion of endothelial cells, facilitating the formation of blood vessels [6–8]. PDGF signaling also appears to regulate the recruitment of support cells (smooth muscle cells/pericytes) to vascular beds [4,9]. Interruption of these angiogenic-associated growth factor receptor tyrosine kinases (RTK) and/or respective signal transduction pathways, therefore, is an appealing target for the development of inhibitors of tumor-mediated angiogenesis. It is in this context that we intend to utilize PD166285 and PD173074 as inhibitors of angiogenic-associated growth factor RTKs and/or signaling pathways involved in tumor vascularization.

The pyrido-[2,3-d]pyrimidine, PD166285, initially was designed to inhibit the catalytic domain of PDGFR-ß TK with the intent of inhibiting PDGF signaling and growth of tumor cells. However, PD166285 was subsequently found to be a potent but rather non-specific inhibitor of other RTKs [10,11]. PD166285 inhibited PDGF-dependent C6 glioma and transformed NIH3T3/PDGF cell growth in a clonogenic assay at nanomolar concentrations [12]. Anti-tumor efficacy (73% reduction in tumor size) was also demonstrated in mice implanted with NIH/3T3/PDGF tumors following oral administration of PD166285 (20 mg/kg; q.d.x14days) [12]. Another, more recently described pyrido-[2,3-d]pyrimidine, PD173074, was rationally synthesized based on the crystal structure of bFGF-inhibitor complex, and not surprisingly, exhibited a high degree of complementarity with the tyrosine kinase domain of $FGFR_1$TK domain [13,14]. $FGFR_1$TK specificity and anti-angiogenic effects of PD173074 on FGF-induced corneal neovascularization were also demonstrated [14].

In our current studies, we examined the pan-RTK inhibitor, PD166285, as well as the selective $FGFR_1$TK inhibitor, PD173074, for their inhibitory effects on angiogenesis and tumor growth both *in vitro* and *in vivo*. More specifically, we set out to determine whether long-term treatment with PD166285 and PD173074 given subsequent to photodynamic therapy (PDT) would greatly improve the duration or extent of anti-tumor efficacy afforded by PDT.

PDT is a biphasic treatment consisting of systemic administration with a photoactivatable drug followed by the focal exposure of a light source at the appropriate wavelength and power to a superficial tumor. It is apparent that activation of the photosensistizing drug produces singlet oxygen which causes oxidative damage to intracellular organelles [15–17]. Much of the evidence suggests the primary target of PDT is the vasculature of the tumor and its destruction inevitably leads to vascular thrombosis, edema and necrosis [18–20].

PDT is currently being evaluated in clinical trial for the treatment of various types of tumors. Most recently, PDT has gained approval in the U.S. for the treatment of early stage lung cancer. It is often a very effective and curative treatment for certain tumors. However, in many instances, the period of tumor regression following PDT is short-lived, even with repeated treatments [21–22]. Many reports demonstrate that vascular damage is temporary. Recent studies show that reperfusion of tissue in experimental models of iris and retinal angiogenesis occurred a few days after PDT [23,24]. Since regeneration of the tumor vasculature is essential for the regrowth of the tumor, suppression of the angiogenic process is greatly warranted. In review of these findings, we felt that PDT offers an opportune circumstance for the additional of secondary therapy that inhibits neovascularization. Since tumor angiogenesis facilitating tumor regrowth could take place at any time after PDT, long-term treatment with anti-angiogenic agents would be necessary to ensure long-term tumor remissions. Therefore, due to the nature of this type of treatment, anti-angiogenic therapies must be relatively non-toxic to the host and not susceptible to drug resistance. In our studies, we evaluated PD166285 and PD173074 first as anti-angiogenic agents and secondly, in combination with PDT in a long-term, maintenance treatment setting.

Methods

Animals. Female C3H mice at least six weeks old were purchased from Clarence Reeder, NCI Fredrick Cancer Research Facility, Fredrick, MD. The mice were housed in the Cancer Cell Center at Roswell Park Cancer Institute and maintained by DLAR employees until needed for experimentation.

Cell lines. Human umbilical vein endothelial cells (HUVEC) (Clonetics Inc., San Diego, CA) were maintained in endothelial cell growth medium (Clonetics Inc., San Diego, CA) for 1–3 passages. In some growth inhibition experiments, HUVEC were also maintained in medium supplemented with 25ng/ml

recombinant human bFGF (UBI, Lake Placid, NY) or 5ng/ml recombinant human VEGF (R & D Systems, Minneapolis, MN). The human breast carcinoma cell lines, MDA435/LCC6 and its MDR transfectant first reported by Leonessa et al. [25], were kindly provided by Dr. R. Clarke (Lombardi Cancer Center, Georgetown University School of Medicine) and were propagated in RPMI-1640 (Life Technologies, Grand Island, NY) containing 5% FCS, 5% NuSerum IV, 20 mM HEPES, 2 mM L-glutamine. The human fibrosarcoma, HT-1080 cell line and its DR4 doxorubicin-selected resistant variant, previously described by Slovak et al. [26], were obtained from Dr. Y. Rustum (Department of Pharmacology & Therapeutics, Roswell Park Cancer Institute) and were grown in RPMI-1640/10% FBS. All lines were grown as monolayers at 37° C in a 5% CO_2 humidified atmosphere.

Tumor models. Before tumor implantation, skin over the right shoulder and rib cage area of C3H mice was shaved and depilated with Nair. The murine mammary 16c tumor, a generous gift from Parke-Davis Pharmaceutical Research, Ann Arbor, MI, was transplanted subcutaneously as a 2 mm^3 fragment with a trocar needle, and tumor size was calculated using the formula $V=(lxw^2)0.4$. Once the tumors reached a size of 1000 mm^3, the mice were sacrificed by cervical dislocation.

Receptor tyrosine kinase assays. Assays using the full length PDGFR-ß-, $FGFR_1$-, EGFR-, insulin-RTK and c-src TK were performed as previously described [10,27]. Briefly, the assay media for TK activity contained 25 mM HEPES buffer (pH 7.4), 150 mM NaCl, 10 mM $MnCl_2$, 0.1 mM sodium orthovanadate, 750 μg/ml of random co-polymer of glutamic acid and tyrosine (4:1), various concentrations of inhibitor and 60–75ng of enzyme. The reaction (total volume, 100 μL) was initiated by the addition of [γ-^{32}P]ATP (50 μM ATP containing 0.4 μCi [^{32}P]ATP per incubation. Samples were incubated for 10 minutes at 25°C and terminated by the addition of 30% trichloroacetic acid. Protein kinase C (PKC) activity was determined as previously described [28].

In vitro growth inhibition assay. PD166285 and PD173074 were synthesized at Parke-Davis Pharmaceutical Laboratories, Ann Arbor, MI and their structures are shown in Figure 1. Assessment of the cellular growth inhibitory effects of PD166285 and PD173074

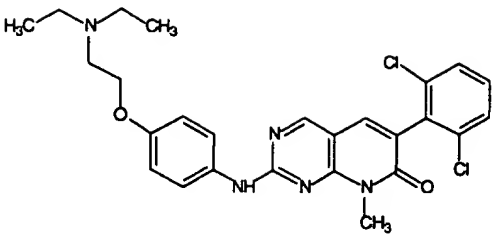

PD 166285

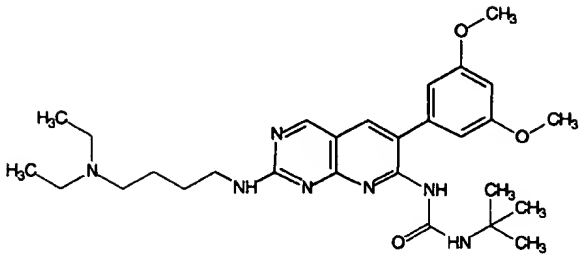

PD 173074

Figure 1. The structures of PD166285 and PD173074. PD166285: 6-(2,6-dichloro-phenyl)-2-[4-(2-diethylamino-ethoxy) -phenylamino]-8-methyl-8H-pyrido[2,3-d]pyrimidin-7-one and PD 173074: 1-tert-butyl-3-{2-(4-dietylamino-butylamino)-6-(3,5-dimethoxy-phenyl)-pyrido[2,3-d]pyrimidin-7-yl}-urea.

were assessed using the sulforhodamine B (SRB) assay according to the methods of Skehan et al. [29]. Briefly, exponentially growing cells were seeded on 96-well microtiter plates and incubated at 37° C for 15–18h to allow attachment of cells prior to drug addition. PD166285 and PD173074 were initially solubilized in DMSO and diluted in RPMI-1640 containing 10 mM HEPES. All cell lines were exposed to 10 different concentrations of drug (5 log range) for 24–72h (2–4 doublings) at 37°C. Cell densities were determined using the sulforhodamine B assay. Data were fit with the Sigmoid-Emax concentration-effect model [30] using nonlinear regression and weighted by the reciprocal of the square of the predicted response. The fitting software was developed at RPCI with MicroSoft FORTRAN, and uses Marquardt algorithm as adapted by Nash [[31] for nonlinear regression. The concentration of drug resulting in 50% growth inhibition (IC_{50}) was estimated.

In vitro microcapillary formation assay. The effects of PD166285 and PD173074 on HUVEC microcapillary formation were determined as previously described [32]. Reconstituted basement membrane,

Matrigel (Collaborative Biomedical Products, Franklin Lakes, NJ), was thawed at 4°C and added to 24-well plates at 250 μg/well and allowed to gel for 1h at 37°C. HUVEC were harvested, resuspended at 1×10^5cells/ml in complete growth medium and seeded on Matrigel-coated 24-wells plates at 5×10^4cells/well. PD166285 or PD173074 was added at non-growth inhibitory concentrations of 0.01, 0.03 and 0.10 μM. Because a 24h incubation is used in this model system, IC_{50} values for a 24h incubation of PD166285 (0.40 μM) and PD173074 (0.30 μM) were determined using the SRB assay. As a positive inhibitory control, suramin, an inhibitor of growth factor mitogenic activity and angiogenesis [33], was also added at nongrowth inhibitory concentrations of 10, 30 and 100 μM (suramin; IC_{50} for 24h was > 100μM). Following a 24h incubation at 37°C, 200 μl (5 mg/ml) of MTT (3-[4,5-dimethylthiazol-2-yl]-2,5-diphenyltetrazolium bromide thiazolyl blue) (Sigma Chemicals Co., St. Louis, MO) was added to each well and incubated at 37°C for 3–4h to visualize viable cells. Microcapillaries were viewed using a light microscope and photographed with a Polaroid camera (Cambridge, MA).

In vivo murine angiogenesis assay. In order to evaluate the inhibitory effects of PD166285 and PD173074 on the formation of blood vessels *in vivo*, we employed a murine angiogenesis assay to assess the growth of blood vessels into subcutaneously implanted Matrigel® [34]. Briefly, 8-week old, female athymic nude mice (Taconic Inc., Germantown, NY) were implanted subcutaneously with 0.5 mg/0.5ml Matrigel that was supplemented with 1.25 μg bFGF (Biosource International Inc., Camarillo, CA) and 60 μg heparan sulfate (Sigma Chemicals Co., St. Louis, MO) and coimpregnated with either PD166285 or PD173074 (10, 30 and 100nM). In subsequent experiments, PD166285 (1–25 mg/kg) or PD173074 (25–100 mg/kg) formulated in 50 mM sodium lactate was administered orally with a feeding needle once a day for 7 days. Positive and negative control groups containing bFGF/heparan sulfate or vehicle in Matrigel, were used for qualitative comparisons. After 7 days, the Matrigel plugs were excised from mice, fixed in 10% formalin, embedded in paraffin, sectioned and stained with Masson's trichrome prior to histologic examination. Tissue sections were examined and photographed with a 35 mm Nikon camera at 40 and 100× magnifications.

Anti-tumor efficacy of photodynamic therapy (PDT) in combination with anti-angiogenic agents. In order to assess the ability of anti-angiogenic agents to improve the duration of anti-tumor response following PDT, experiments utilizing a combination of PDT [35] and anti-angiogenic agents were performed. Mice were implanted with murine mammary 16c tumor as described previously [35]. After 4–6 days when tumors were approximately 50–100 mm^3, hexylether pyropheophorbide-a, a novel photosensitizer with less long-term normal tissue phototoxicity than Photofrin ® [36], was formulated in sterile water/5%dextrose/1%tween-80, and a 0.3 μmol/kg dose was administered intravenously (i.v.). After 24hr, the tumors were exposed for 30 min to a light beam (1 cm treatment field diameter; dose rate 75mW/cm^2) at a wavelength of 665 nm and light surface dose of 135J/cm^2 from an argon-ion laser (Model 171, Spectra-Physics, Mt. View, CA). On the next day, PD166285 (5–10 mg/kg) or PD173074 (30–60 mg/kg) were administered p.o. daily with a feeding needle for a period $\leq$28 days. To compare the efficacy of these RTK inhibitors to another anti-angiogenic agent, we employed suramin (40–80 mg/kg), a potent antagonist of heparan-binding growth factors. Suramin was administered intraperitoneally for a period of 9 days following PDT. Tumor volumes were measured with calipers and mice were weighed continuously. Mice were sacrificed when tumors reached 1000 mm^3. Delays in tumor regrowth following PDT, time to reach 1000 mm^3 and numbers of long-term survivors (complete tumor remission >30 control tumor volume doubling time in days) were assessed and considered in the evaluation of anti-tumor efficacy.

Histology. The histology service laboratory at RPCI in the Grace Cancer Drug Center performed all tissues prepared for histological analysis.

Results

The objective of this study was to evaluate the effects of a potent, broadly active RTK inhibitor, PD166285 and a highly selective $FGFR_1$TK inhibitor, PD173074, on endothelial cell growth, microcapillary formation *in vitro* and *in vivo*, and tumor regrowth following PDT. The ability of these compounds to inhibit RTKs such as the receptors for PDGF, EGF, and specifically, bFGF provided the rationale for assessing their anti-angiogenic potential.

Table 1. Effects of PD166285 and PD173074 on kinase activity[a]

Compound	PDGFR-βTK IC_{50} (μM)	$FGFR_1TK$ IC_{50} (μM)	C-SRC TK IC_{50} (μM)	EGFRTK IC_{50} (μM)	Insulin-RTK IC_{50} (μM)	PKC IC_{50} (μM)
PD 166285	0.085± 0.019	0.038 ± 0.009	0.007 ± 0.005	0.035	>50	22.7
PD 173074	15.5 ± 2.7	0.026 ± 0.004	20.3 ± 4.5	>40	>50	>40

[a] Kinase activity was measured as previously described [10,11,16]. IC_{50} values represent the concentration of compound that inhibited enzyme activity by 50% and are the mean of 3 or more experiments performed in triplicate ± SD. IC_{50} values without indicated SD are the mean of 2 experiments performed in duplicate.

Table 2. Effects of PD166285 and PD173074 on cell growth[a]

Compound	HUVEC	IC50 (μM) LCC6-WT	± LCC6-MDR	S.E.[b] HT-1080	HT-1080/DR4
PD166285	0.12 ± 0.004	0.14 ± 0.002	0.14 ± 0.002	0.28 ± 0.01	0.28 ± 0.01
PD173074	0.06 ± 0.008	11 ± 0.16	12 ± 0.106.4 ± 0.13	6.8 ± 0.55	

[a] Human cell lines: HUVEC – human umbilical vein endothelial cells; Human breast, MDA-435 LCC6-WT and MDR1 transfected carcinoma cell lines; Human fibrosarcoma HT-1080 and HT-1080-DR4 (doxorubicin-selected, MRP positive) cell lines.
[b] Exposure time equals 100 h for HUVEC and HT-1080/DR4 (~3.5 cell doublings) and 72 h for LCC6-WT, LCC6-MDR and HT-1080 (~3.3 cell doublings). All assays contained six replicate wells and were performed on at least three separate occasions. Mean and standard deviation are given.

To verify RTK specificity of PD166285 and PD173074 that has already been established, we performed RTK assays as previously described [10,13,14,27]. PD166285 potently inhibited several tyrosine kinases including c-src, $FGFR_1$, PDGFR-ß and EGFR with IC_{50}values as low as 7nM (Table 1). PD166285 had no effect on PKC activity at concentrations as high as 40 μM and also has no effect on insulin RTK at concentrations as high as 50 μM. In contrast, PD173074 displayed an almost 1000-fold selective inhibition toward $FGFR_1TK$, with an IC_{50} of 26nM, whereas against other tyrosine kinases or PKC, the IC_{50} values were 15 μM or greater (Table 1).

Effects of PD166285 and PD173074 on the growth of human endothelial and tumor cell lines were evaluated to assess cell selectivity. Tumor cell variants possessing multi-drug resistant phenotypes were also included in the panel of cell types to assess the potential for anti-tumor drug resistance. PD166285 did not show any differential growth inhibitory effects between HUVEC (IC_{50};0.12 μM) and several tumor cell lines (IC_{50};0.10–0.28 μM) (Table 2). However, PD173074 was 100–200 fold more selective in inhibiting HUVEC growth (IC_{50};0.06 μM) as compared with the growth of various tumor cell lines (IC_{50};6.4–12.1 μM) (Table 2). PD173074 was also about two-fold more active in its growth inhibitory action on HUVEC (IC_{50};0.06 μM) compared with PD166285 (IC_{50};0.12 μM) (Table 2). In addition, the LCC6-MDR and HT-1080 DR4 drug resistant lines overexpressing drug efflux pumps, P-glycoprotein and multidrug related protein (MRP), respectively, did not display any cross-resistance to PD166285 or PD173074.

Inhibition of HUVEC growth by PD166285 and PD173074 was further examined in which we performed growth inhibitory studies on HUVEC grown in the presence of either bFGF or VEGF. Manipulating HUVEC growth medium in this manner created a circumstance in which HUVEC growth was stimulated exclusively by either bFGF or VEGF. PD166285 or PD173074 treatment under these conditions helped clarify RTK target specificity. As noted by the data, it appeared that PD173074 specifically inhibited the growth of bFGF-stimulated HUVEC growth (IC_{50};0.007 μM) and was less active against VEGF-stimulated HUVEC growth (IC_{50};0.194 μM) (Table 3). PD166285, on the other hand, inhibited both bFGF and VEGF-stimulated HUVEC equally (IC_{50};0.028 and 0.037 μM, respectively) (Table 3). These data suggest that PD173074 more specifically inhibited bFGF-related RTK in comparison to VEGF-related RTK, while PD166285 appeared to equally

Table 3. Effects of PD166285 and PD173074 on HUVEC growth[a]

Compound	IC_{50} (μM)[b] bFGF-supplementation	VEGF-supplementation
PD 166285	0.028	0.037
PD 173074	0.007	0.194

[a]HUVEC were grown for 4 days in the presence or absence of the indicated compound in HUVEC-conditioned media containing either 5 ng/ml VEGF or 25 ng/ml bFGF.
[b]IC_{50} values are the concentration that inhibits 50% of the stimulated growth by either bFGF or VEGF and are the mean of 3 or more experiments performed in triplicate.

interrupt both bFGF- and VEGF-related RTKs associated with HUVEC growth.

Based on the cellular growth inhibitory properties of PD166285 (IC_{50};0.40 μM) and PD173074 (IC_{50};0.30 μM) over a 24hr incubation (data not shown), we employed low, *non*-growth inhibitory concentrations in evaluating their effects on angiogenesis, *in vitro*. This treatment approach allowed for an assessment of these agents' specific anti-angiogenic properties irrespective of growth cessation. Using an *in vitro* microcapillary formation assay, we assessed the ability of these compounds to inhibit the formation of a capillary network produced by HUVEC grown on a reconstituted basement membrane, Matrigel®. HUVEC capillary network formation was inhibited at concentrations as low as 0.01 μM by both agents, with PD166285 being slightly more potent at high concentrations (See Figure 2). Suramin, used for comparison, also inhibited HUVEC capillary formation but at a 1000-fold higher concentration (Figure 2).

Effects of PD166285 and PD173074 on the development of new blood vessels/neovascularization, *in vivo*, were investigated using a murine angiogenesis model [34]. This model utilizes a subcutaneous implant of reconstituted basement membrane (Matrigel) impregnated with bFGF/heparan sulfate, which forms a solid, gelatinous plug capable of providing an appropriate extracellular/stromal environment for the development of functional vasculature. Although not well defined, Matrigel is derived from the stromal component of the Engelbreth-Holm-Swarm (EHS) murine sarcoma and relevant for studies focused on tumor angiogenesis [37]. The most common components of Matrigel include laminin, heparan sulfate proteoglycans and collagens along with growth factors, which facilitate the acquisition of invasive and migratory properties of endothelial cells and other cells of mesenchymal origin.

In our initial studies in mice, we added the same concentrations of PD166285 and PD173074 to the implanted Matrigel plugs that were effective in the *in vitro* microcapillary formation assay. Angiogenesis, in this model system, is characterized by the migration of blood vessels into the bFGF/heparan- impregnated, s.c. implanted Matrigel plug. Histological examination of Matrigel plug sections revealed the presence of bright red stained cells (erythrocytes, endothelial, fibroblast and smooth muscle cells) and red circular structures (blood vessels/capillaries) against a bluish-green stained Matrigel background which varied from batch to batch (Figure 3, Panel G, 100×). This positive angiogenic state was compared with Matrigel plugs lacking bFGF/heparan which did not show any influx of capillaries within the entire area of the section (Figure 3, Panels A, 40×; and D, 100×). When PD166285 or PD173074 were coimpregnated into the Matrigel, a concentration-dependent inhibition of angiogenesis was observed (Figure 3). PD166285 appeared to be more potent, partially inhibiting angiogenesis at 0.01 μM (Figure 3, Panel B) and completely inhibiting capillary formation at higher concentrations (Panels E and H). PD173074, on the other hand, did not demonstrate any inhibitory activity at 0.01 μM; however, at higher concentrations, it worked as well as PD166285 (Panels F and I).

Since PD166285 and PD173074 were found to be orally bioavailable, they were administered in a 50 mM sodium lactate formulation to assess the ability of these agents to inhibit angiogenesis within a bFGF/heparan impregnated Matrigel plug. These agents were administered p.o. daily for seven days. No acute or cumulative drug toxicity as indicated by mouse weight was noticed during the duration of the experiments using PD166285 at 1 and 5 mg/kg/d × 7 or PD173074 at 25 and 50 mg/kg/d × 7. Representative micrographs of Matrigel sections of PD166285- and PD173074- treated mice demonstrated a dose-dependent anti-angiogenic effect (Figure 4; Panels B, E and H and panels C, F and I, respectively). PD166285 was more active (maximal inhibition of angiogenesis was noted at 5 mg/kg) (Figure 4; Panel E) than PD173074, reflecting its ability to inhibit several RTKs and interrelated angiogenesis signaling pathways.

To assess the anti-tumor efficacy of these potent anti-angiogenic agents in mice, we utilized them in

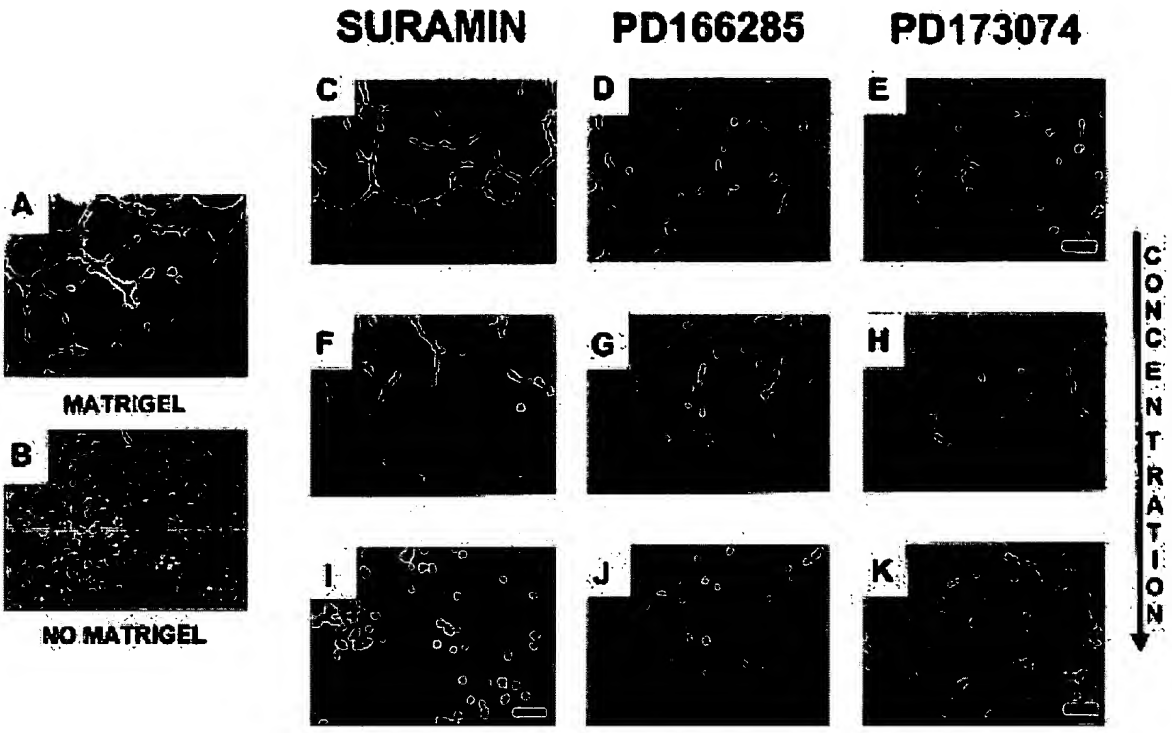

Figure 2. Microcapillary formation assay. Effects of PD166285 and PD173074 on the formation of microcapillaries by HUVEC grown on Matrigel-coated plastic for 24h were evaluated. Please note that the IC_{50} values for a 24h incubation with PD166285 and PD173074 were 0.40 μM and 0.30 μM, respectively (data not shown), with inhibition to HUVEC growth observed at the highest concentrations (0.1 μM) tested for 24h in this assay. Microcapillary networks were observed after staining HUVEC with MTT. In Panel A, a representative culture of HUVEC grown on Matrigel for 24h; note the extensive formation of a microcapillary network (40×). Panel B – no Matrigel (100×). Panels C, F and I represent HUVEC exposed to 10, 30, and 100 μM Suramin, respectively (40×). Note the disappearance of the microcapillary network following the addition of either 30 or 100 μM Suramin. Panels D, G and J represent 0.01, 0.03 and 0.10 μM PD166285 (40×), while Panels E, H and K illustrate 0.01, 0.03 and 0.10 μM PD173074 (40×). Note the concentration-dependent, inhibition of capillary network formation in the PD166285 and PD173074 groups. All experiments were performed in triplicate on three separate occasions. Magnification bars; Panel B=120 μm and Panels A, C-K=300 μm.

an adjuvant setting given subsequent to cytoablative treatment, photodynamic therapy (PDT).

All mice were implanted subcutaneously with a murine mammary 16c tumor and treated with PDT and/or PD166285 and PD173074 as described in the Materials and Methods. Mice treated with PDT alone or suramin (40 or 80 mg/kg) showed no significant increase in tumor growth delay when compared with the control untreated group (Table 4). However, combining PDT (0.3 mg/kg,HPPH; 665 nm; 135J/cm^2 for 30 min) and follow-up treatment for 14 days with PD166285 (10 mg/kg) or PD173074 (30 or 60 mg/kg) displayed a dramatic increase in tumor-free interval (Figure 5). In addition, most animals treated with PDT in combination PD166285 (10 mg/kg) and PD173074 (30 mg/kg) for 28 days displayed even greater tumor growth delays (Figure 5). As outlined in Table 4, median times for tumors to reach 1000 mm^3 in the PDT combined with PD166285 or PD173074, or PD166285 or PD173074 alone groups were prolonged when compared with the PDT alone group. Tumor growth delays in PDT combined with PD166285 or PD173074, or PD166285 or PD173074 alone groups were statistically greater than PDT treatment alone groups ($\geq$13 days, $p<0.001$, Cox-Mantel Test). Interestingly, only mice from the combination treatment groups exhibited cures, but the length of follow-up treatment with either PD166285 or PD173074 from 14 to 28 days did not significantly improve the cure rate. In most cases, tumors began to regrow about a week after withdrawal from both 14- and 28-day treatment periods strongly suggesting the need to employ maintenance-type treatments with these types of agents.

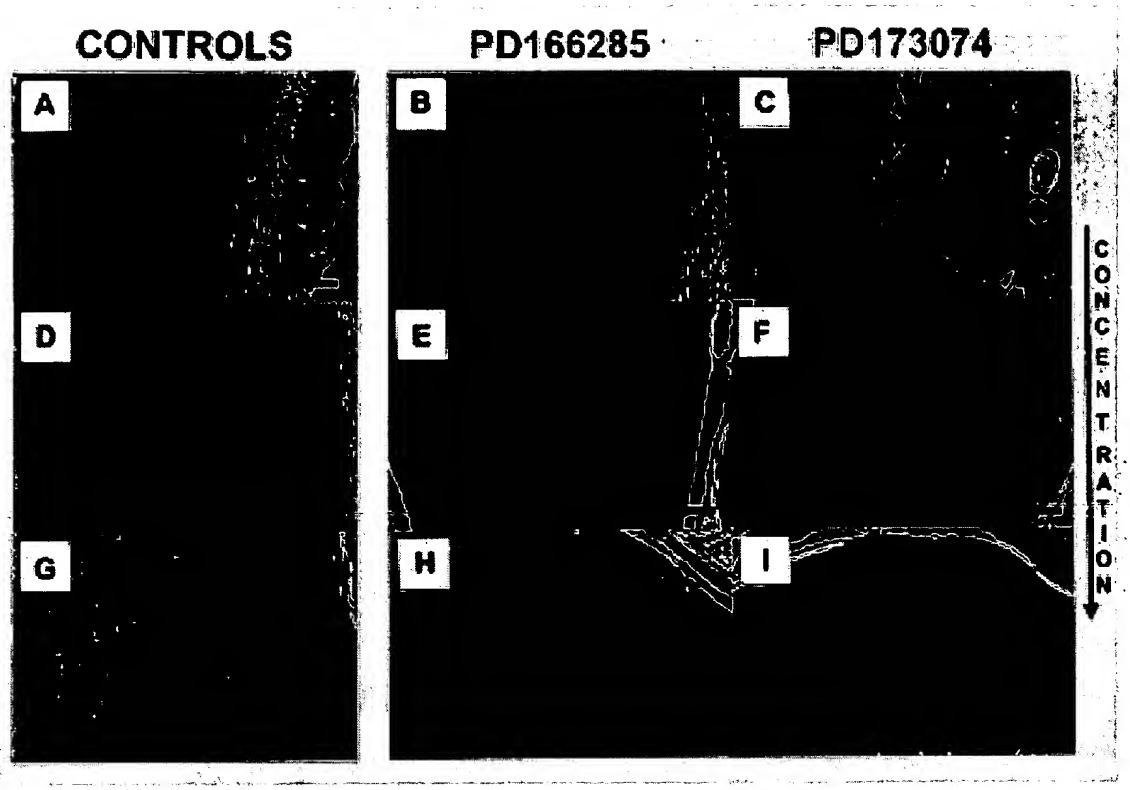

Figure 3. In vivo murine angiogenesis assay. PD166285 and PD173074 were evaluated for their ability to inhibit murine angiogenesis in a subcutaneously implanted Matrigel plug. Matrigel plugs (0.5 mg/0.5ml/plug) were supplemented with 1.25 μg bFGF/60 μg heparan-sulfate, and in some cases coimpregnated with PD166285 or PD173074, and implanted subcutaneously into athymic nude mice. Matrigel plugs were resected after 7 days, embedded in paraffin, sectioned and stained with Masson's trichrome. Representative micrographs of duplicates from control and treated groups are illustrated. Matrigel without bFGF/heparan sulfate, Panels A (40×) and D (100×); Matrigel coimpregnated with bFGF/heparan sulfate, Panel G (100×). Note the large influx of endothelial/mesenchymal cells and the formation of numerous blood vessels; Drug treatment groups, Panels B, E and H – 0.01, 0.03 and 0.10 μM PD166285 (100×), Panels C, F and I – 0.01, 0.03 and 0.10 μM PD173074 (100×). Note the suppression of angiogenesis in drug-treated groups. Magnification bars: Panel A=250 μm and Panels B-I=100 μm.

In addition to the efficacy generated in these combination treatment studies, we also observed some side effects unrelated to weight loss associated with PD166285 treatment. Because PDT created an abscess over 16c tumors, wound healing following PDT was an active process. However, wound healing in the presence of PD166285 (5–10 mg/kg q.d. $\leq$ 28 days) was abnormal; a hyperplasia emerged in the area of the abscess. Histologic analysis of the skin lesion revealed that it was hyperkeratosis (Figure 6B). Following withdrawal of PD166285 treatment, the lesions disappeared. Also, 20% of the mice that were treated with PD166285 for 28 days experienced neurotoxicity that resulted in their demise unrelated to tumor burden. PD173074 treatment, contrary to the side effects observed with PD166285 treatment, did not manifest any noticeable toxicities.

Discussion

There is overwhelming evidence suggesting that angiogenesis, the process by which new blood vessels are formed from preexisting vessels, occurs concurrent with tumor growth and progression [38,39]. Angiogenesis that occurs within tumors is often characterized by proliferation, invasion and migration of neighboring endothelial cells and other blood vessel-related cells including smooth muscle cells (pericytes) requisite for blood vessel generation and maintenance. Chemotactic signaling involved in this phe-

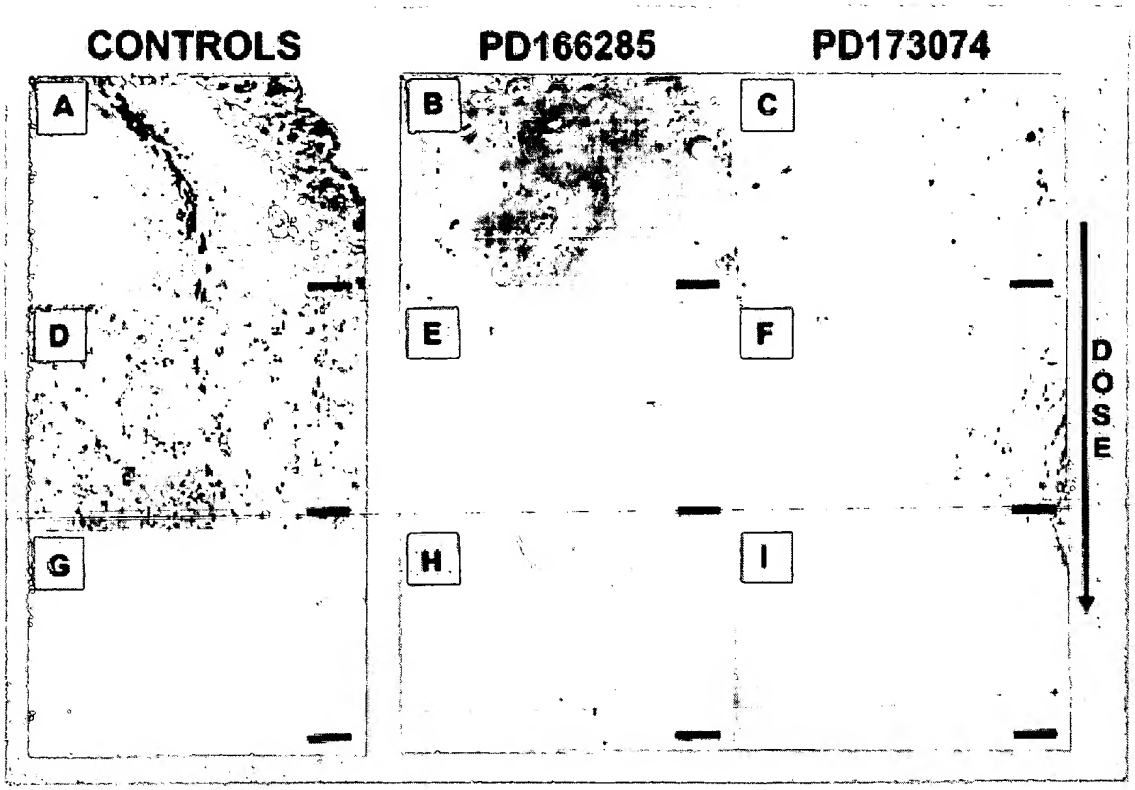

Figure 4. In vivo drug administration and murine angiogenesis assay. Orally administered PD166285 and PD173074 were evaluated for the ability to inhibit murine angiogenesis in a subcutaneously implanted Matrigel plug. Matrigel plugs (0.5 mg/0.5ml/plug) were supplemented with 1.25 μg bFGF/60 μg heparan sulfate and implanted subcutaneously into athymic nude mice. Mice were administered PD166285 or PD173074 formulated in 50 mM sodium lactate, p.o., once a day for 7 days. Matrigel plugs were resected after 7 days, embedded in paraffin, sectioned and stained with Masson's trichrome. Representative micrographs of duplicates from control and drug-treated animal groups are as follows: Matrigel plug with bFGF/heparan sulfate, Panels A (40×) and D (100×), and without bFGF/heparan sulfate, Panel G (100×). Drug treatment groups all containing bFGF/heparan sulfate, Panels B, E and H – 1, 5 and 25 mg/kg PD166285 (100×) and Panels C, F and I – 25, 50 and 100 mg/kg PD173074 (100×). Note the extent of angiogenesis in the positive control (Panel D) as evidenced by cellularity and extent of capillary formation, as well as anti-angiogenic efficacy of drug treatment [PD166285 (Panels B, E and H) and PD173074 (Panels C, F, and I)]. Magnification bars: Panel A=250 μm and Panels B-I=100 μm.

nomenon is controlled by paracrine growth factors, which interact with specific ligand binding domains of transmembrane receptor tyrosine kinases (RTK). This interaction modulates tyrosine kinase activities that ultimately mediate the induction of vascular cell proliferation and differentiation. Some recent observations from studies using transgenic mice lacking specific RTKs such as vascular endothelial growth factor receptors VEGFR-1/2, platelet-derived growth factor receptors PDGFR-α/ß and fibroblast growth factor receptor $FGFR_1$ suggest that these receptors are essential for vasculogenesis, normal vascular development and mesodermal patterning, respectively [40–44]. The ability of activated RTKs to elicit angiogenesis, therefore, offers an opportune target for exploitation using inhibitors of RTKs with potential anti-angiogenic and anti-tumor implications.

In this study, we demonstrated the ability of PD166285 to equally inhibit a panel of TKs and PD173074 to selectively inhibit $FGFR_1$TK. To date, efforts have been made to synthesize and evaluate compounds with RTK inhibitory activity as potential anti-tumor agents [45–47]. The use of these compounds as anti-angiogenic agents, however, is in its infancy. Our studies demonstrated the efficacy of PD166285 and PD173074 as anti-angiogenic agents in preclinical murine models (Table 5). These data included the demonstration of dose-dependent sup-

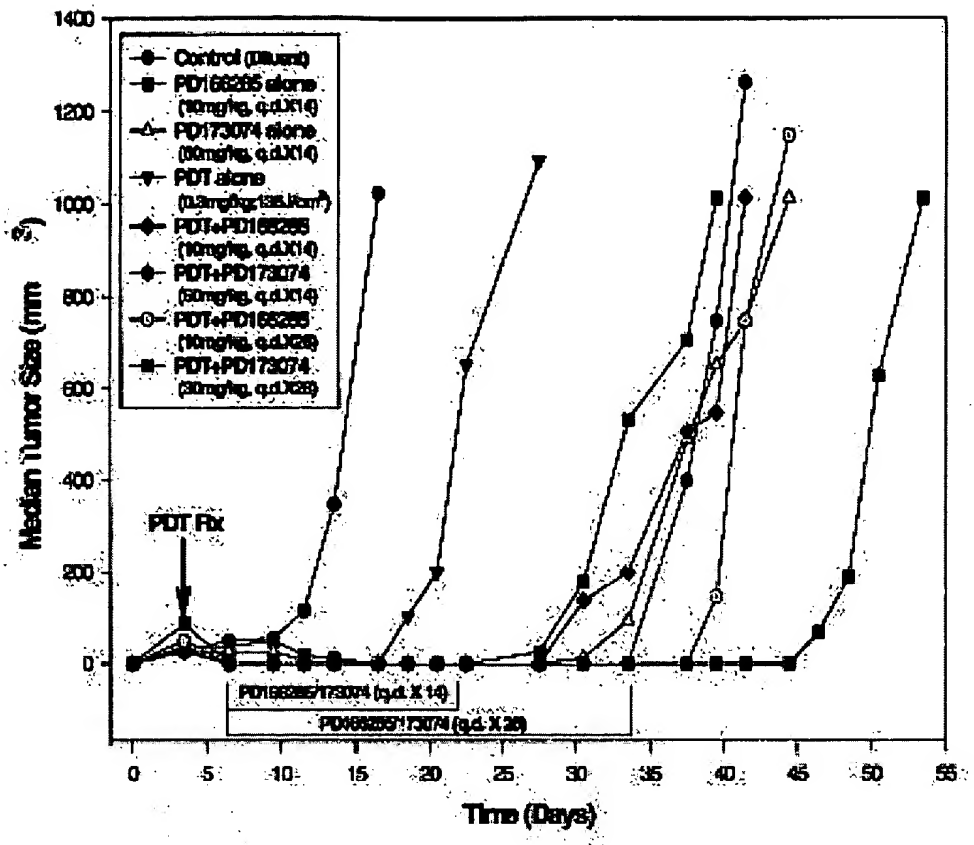

Figure 5. Anti-tumor activity of PDT in combination with PD166285 or PD173074 against a murine mammary 16c tumor. Please refer to the legend for symbols corresponding to the growth of the tumor over time. Note the point at which the PDT treatment was initiated, and following complete regression, the regrowth of the tumors shortly after withdrawal of the drug. PD166285 and PD173074 treatment commenced following PDT and was continued q.d. for 14 or 28 days.

gression of angiogenesis and a 1000-fold increase in HUVEC sensitivity to the agents compared with suramin, a well-characterized anti-angiogenic agent. Furthermore, the lack of apparent host toxicity associated with systemic treatment of these agents at efficacious doses implied the beneficial use of these agents as cytostatic adjuvants to conventional treatment modalities [48,49]. Because tumor growth, metastasis and recurrence following cytoreductive therapies may be dependent on angiogenesis, follow-up treatment with angiogenesis inhibitors such as PD166285 and/or PD173074 may need to be long-term, in a maintenance-type setting [50–52]. However, recent studies in mice with the potent angiogenic inhibitor, endostatin, have demonstrated that after serial treatment regimens, tumors completely regressed with no apparent tumor regrowth or acquired resistance [53].

The cancer treatment paradigm that we put forth employed a combination of photodynamic therapy (PDT) followed by anti-angiogenic therapy [35]. Currently, PDT, which results in the destruction of the tumor vasculature, is being evaluated in a clinical setting [54]. It has been shown to be effective against local recurrent breast tumors [55,56] and malignant, tumors of the skin [57], esophagus [58], bladder [59] and bronchus [60,61]. Duration of response to PDT, although, is often short-lived due to the rapid regrowth of the tumor. Early evidence from our laboratory showed that paclitaxel or suramin at anti-angiogenic doses, when given in combination with PDT against human breast tumor xenografts in nude mice, res-

Table 4. Anti-tumor efficacy of PDT in combination with PD166285 or PD173074 against a murine nammary 16c tumor*

Treatment	Dosage[a] (mg/kg)	Median tumor growth[b] & growth delay following PDT (days)		Long-term survivors[c]
Control	–	17	–10	0/21
PD166285 alone	10	39	13**	0/6
PD173074 alone	60	44	18**	0/6
Suramin alone	40	18	0	0/6
Suramin alone	80	25	–1	0/6
PDT alone	–	26	–	0/19
PDT+Suramin	40	26	0	0/7
PDT+Suramin	80	30	4	0/7
PDT+PD166285	10	41	15**	2/7
PDT+PD166285	10[d]	43	17**	1/8***
PDT+PD173074	60	40	14**	1/8
PDT+PD173074	30[d]	53	27**	1/8

[a]PDT consisted of an i.v. dose of 0.3 mg/kg HPPH; and after 24hr, tumors were exposed to a focal light beam (665 nm, 135J/cm^2) for 30 min. PD166285 (10 mg/kg)/PD173074 (60 mg/kg) and suramin were administered orally in a 50 mM Na^+ Lactate solution for 14 days and 9 days, respectively, following PDT.
[b]Time required for median tumor to reach 1000 mm^3 and growth delay following PDT.
[c]Mice showed no detectable tumor for >30× control tumor doubling time (3 days).
[d] PD166285 (10 mg/kg) and PD173074 (30 mg/kg) were administered orally for 28 days following PDT.
*Data taken from two separate experiments.
**Comparison with PDT alone group (Cox-Mantel test); $p < 0.001$.
***Two mice exhibited neurotoxicity, and although showed no detectable tumor, were not included in statistical comparisons.

ulted in increased tumor growth delay with a large percentage of the mice remaining tumor free [35].

In our recent studies, initial ablation of murine mammary 16c tumors with PDT and subsequent anti-angiogenic treatment consisting of well-tolerated doses of PD166285 and PD173074 suppressed tumor regrowth and lengthened the time of complete tumor remission. Remarkably, use of these RTK inhibitors in combination with PDT also generated long-term survivors in 17% of the mice. Interestingly, cessation of PD166285 or PD173074 treatment after 14 days resulted in almost immediate tumor regrowth reinforcing our idea that these cytostatic anti-angiogenic therapies need to be administered long-term, or even life-long, to control tumor regrowth (Figure 5). Likewise, in those mice that received drug treatment for 28 days following PDT, treatment with PD173074 (30 mg/kg) or PD166285 (10 mg/kg) sustained complete tumor regression in the presence of the drug until shortly after withdrawal of drug.

In general, murine mammary 16c tumor was sensitive to RTK inhibitor treatment as noted by tumor regression and maintenance of complete regression following PDT in the presence of PD166285 or PD173074 *alone* (Figure 5). *In vivo* sensitivity of this tumor to PD166285 or PD173074 treatment may have been due to effects on mammary 16c tumor-associated endothelial cells and not due to inherent sensitivity of the tumor cell itself. Levels of specific angiogenic growth factors released either directly by this tumor or indirectly via tumor-secreted proteases may help explain for its sensitivity. Since we could not generate mammary 16c cultures *in vitro*, we could not assess a direct effect of PD166285 or PD173074 on mammary 16c tumor cell growth. However, weaker growth inhibitory effects by PD173074 on human breast cancer and fibrosarcoma (Table 2; IC_{50}=11 μM and 6.4, respectively) compared with higher potency against endothelial cells (Table 2; IC_{50}=0.06 μM) suggested that anti-tumor activity of RTK inhibitors was due to an anti-vascular response. In any event, the efficacy of RTKI administration, whether due to its antiangiogenic activity and direct antitumor activity, appear to be additive to the therapeutic benefit of PDT.

To demonstrate that anti-angiogenesis resulted in anti-tumor efficacy, we attempted to assess blood vessel density in tumors from control and combination treated mice by detecting endothelial-specific

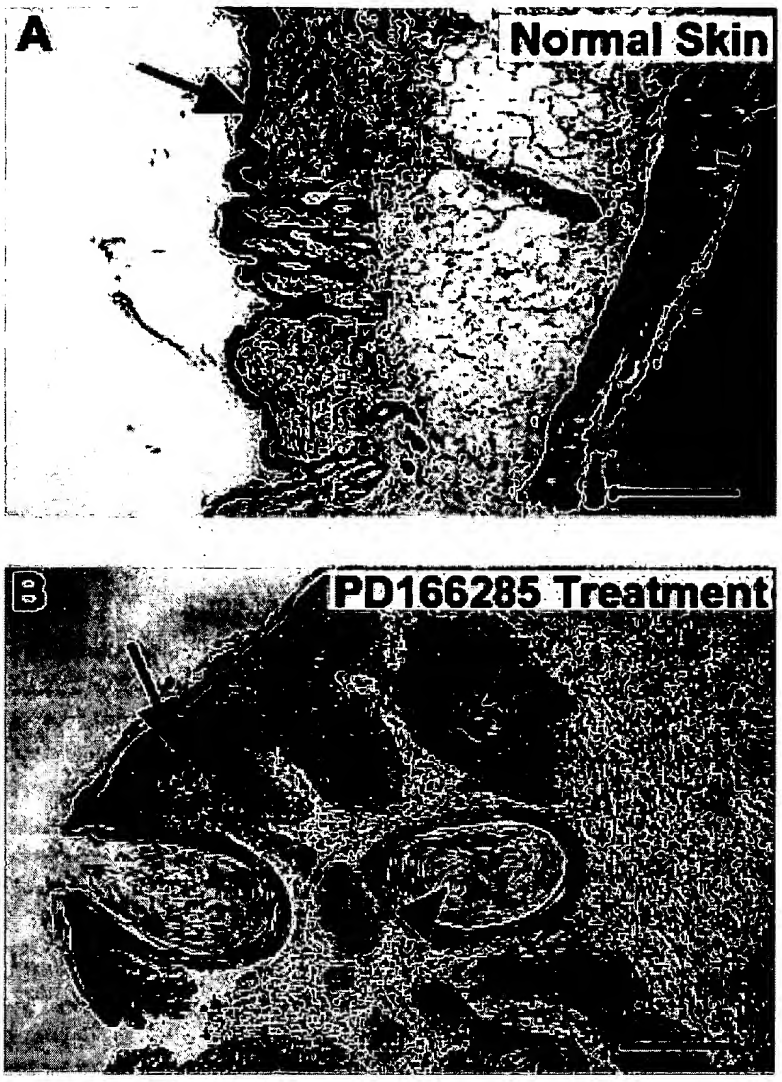

Figure 6. Hematoxylin and eosin (H and E) stained sections of normal skin and hyperkeratosis. Normal skin (Panel A) and a lesion caused by PD166285 treatment (Panel B) in the wound left by PDT were resected, fixed in 10% Formalin, embedded in paraffin, sectioned and stained with H and E. Note the thickening of the epithelial layer (arrow) in Panel B in comparison to Panel A and hyperkeratin (arrowhead) in Panel B. Magnification bar = 200 μm.

molecules, CD31 and CD34, to help identify micro- and macrocapillaries. Unfortunately, we could not detect murine CD31 or CD34 in mammary 16c tumors, but observed their presence in peri-tumor tissue (data not shown). If we recall, those mice bearing mammary 16c tumors that exhibited complete regressions to RTK inhibitor treatment did not possess a tumor. Thus, tumor tissue was not available for histologic examination. This circumstance did not allow for a blood vessel density comparison between tumors from control and drug treated mice. Those tumors that relapsed following PD166285 or PD173074 treatment termination grew to the same size at a similar rate as control tumors. The above evidence strongly suggested that an anti-angiogenic effect rather than a direct anti-tumor effect was responsible for anti-tumor efficacy.

Due to the abscess ($\sim$ 1 cm^2) caused by the focal exposure to the light source after this second phase of PDT, we conceived that the healing of this wound, which is dependent on angiogenesis, would be inter-

Table 5. Summary of the inhibitory effects of PD166285 and PD173074 on *in vitro* and *in vivo* angiogenesis[a]

Compound (μM)	*in vitro* microcapillary formation assay	*in vivo* murine angiogenesis assay Coimpregnated	Oral treatment (mg/kg/d)[c]
Suramin			
10	–	n/d[b]	n/d
30	+	n/d	n/d
100	+++	n/d	n/d
PD166285			
0.01	+	+	+ (1)
0.03	++	+++	+++ (5)
0.10	+++	+++	+++ (25)
PD173074			
0.01	+	–	+ (25)
0.03	++	++	++ (50)
0.10	++	+++	+++ (100)

[a]The extent of inhibition of microcapillary formation by HUVEC grown on Matrigel-coated plastic was scored on replicate plates in double-blind manner and designated as follows: none (–), slight (+), moderate (++) or strong (+++) inhibition. The degree of *in vivo* murine angiogenesis within Matrigel plugs was scored in a similar manner.
[b]n/d-not determined.
[c]p.o. daily × 7.

rupted during follow-up treatment with PD166285 or PD173074. In the case of PD166285 treatment, the healing process seemed to be active but a hyperplastic lesion over the surface of the wound had developed that was characterized by hematoxylin and eosin staining as a hyperkeratotic state (Figure 6B). This keratinized hyperplastic lesion did not contain hair follicles and remained present until shortly after PD166285 treatment. Furthermore, 2 out of 10 mice treated for 28 days with PD166285 (10 mg/kg) developed unilateral paralysis suggestive of neurotoxicity. PD173074 treatment, on the other hand, did not affect wound healing nor cause any adverse side effects at therapeutic doses.

In conclusion, PD166285 and PD173074 displayed potent anti-angiogenic and anti-tumor activity in combination with PDT. Our findings demonstrated that these agents are capable of inhibiting angiogenic-associated receptor tyrosine kinases and angiogenesis. Oral bioavailability and well-tolerable doses of these RTK inhibitors allowed for their use as cytostatic adjuvants when administered in combination with cytoreductive therapy, PDT. It appeared that the specific RTK inhibitor, PD173074, was better than the more broadly active inhibitor, PD166285, in terms of therapeutic index and overall anti-tumor efficacy. Furthermore, tumor cell sensitivity and responsiveness to RTK inhibitors as well as dependence on vascularization will most likely impinge on the effectiveness of RTK inhibitor treatment. Ongoing preclinical testing of these agents in other treatment paradigms and model systems will provide the rationale and further bases for the development of these agents to clinical trial.

Acknowledgments

We thank Mary Vaughan, Department of Pharmacology and Therapeutics, Roswell Park Cancer Institute for providing histology service and Dr. K. Toth for his interpretation of the histological sections. We also graciously thank Drs. A. Kraker, D. Fry and R. Panek from Parke-Davis for their performance of kinase assays. A special thanks is extended to Drs. J. Azizkhan, C. Porter and J. Black for their critical review of this manuscript. These studies were supported in part by NIH grant CA70853 (RJB), CA73872 (RJB). and an Institutional Core Grant, CA-16056 at RPCI.

References

1. Tronick SR, Aaronson SA: Growth factors and signal transduction. In: J. Mendelsohn, P. M. Howley, M. A. Israel and L. A. Liotta editors. The Molecular Basis of Cancer. Philadelphia: W.B. Saunders Co.: p. 117–40, 1995
2. Merenmies J, Parada LF, Henkemeyer M: Receptor tyrosine kinase signaling in vascular development. Cell Growth Diff 8: 3–10, 1997
3. Risau W: Mechanisms of angiogenesis. Nature, 386(17): 671–74, 1997
4. Beck L Jr, D'Amore PA: Vascular development: cellular and molecular regulation. FASEB J 11(5): 365–73, 1997
5. Plate K H, Breier G, Weich HA, Risau W: Vascular endothelial growth factor is a potential tumour angiogenesis factor in human gliomas in vivo. Nature 359: 843–45, 1992
6. Fernig DG, Gallagher JT: Fibroblast growth factors and their receptors: an information network controlling tissue growth, morphogenesis and repair. Prog Growth Factor Res 5(4): 353–77, 1997
7. Klagsbrun M, D'Amore PA: Vascular endothelial growth factor and its receptors. Cytokine Growth Factor Rev 7(3): 259–70, 1996
8. Battegay EJ, Rupp J, Iruela-Arispe L, Sage EH, Pech M: PDGF-BB modulates endothelial proliferation and angiogenesis in vitro via PDGF ß-receptors. J Cell Biol125(4): 917–28, 1994

9. Rohovsky SA, Hirschi KK, D'Amore PA: Growth factor effects on a model of vessel formation. Surg Forum 47: 390–91, 1996
10. Panek RL, Lu GH, Klutchko SR, Batley BL, Dahring TK, Hamby JM, Hallak H, Dohert AM, Keiser JA: In vitro pharmacological characterization of PD166285, a new nanomolar potent and broadly active protein tyrosine kinase inhibitor. J Pharm Exp Thera 283(3): 1433–44, 1997
11. Connolly CJ, Hamby JM, Schroeder MC, Barvian M, Lu GH, Panek RL, Amar A, Shen C, Kraker AJ, Fry DW, Klohs WD, Doherty AM: Discovery and structure-activity studies of a novel series of pyrido[2,3-D]pyrimidine tyrosine kinase inhibitors. Bioorg Med Chem Letters 7(18): 2415–20, 1997
12. Klohs WD, Steinkamph R, Driscoll D, Klutchko SR, Hamby, J, Lu GH, Vincent P, Roberts B, Elliott WL: Characterization of PDGF tyrosine kinase inhibitors in in vitro and in vivo tumors. Proc Amer Ass Can Res 38: 632, 1997
13. Hamby JM, Connolly CJ, Schroeder M, Winters R, Showalter H, Panek RL, Major T, Olsewski B, Ryan M, Dahring TK, Lu G, Keiser JA, Amar A, Shen C, Kraker AJ, Slintak V, Nelson JM, Fry DW, Bradford L, Hallak H, Doherty A M: Structure-activity relationships for a novel series of pyrido[2,3-D]pyrimidine tyrosine kinase inhibitors. J Med Chem 40(15): 2296–303, 1997
14. Mohammad M, Froum S, Hamby JM, Schroeder MC, Panek RL, Lu GH, Eliseenkova AV, Green D, Schlessinger J, Hubbard SR: Crystal structure of an angiogenesis inhibitor bound to the FGF receptor tyrosine kinase domain. EMBO J. 17(20): 5896–904, 1998
15. Weishaupt KR, Gomer CJ, Dougherty TJ: Identification of singlet oxygen as the cytotoxic agent in the photoactivation of a murine tumor. Cancer Res 36: 2322–29, 1976
16. Kessel D: Sites of photosensitization by derivatives of hematoporphrin derivative. Photochem Photobiol 44: 489–93, 1986
17. Gibson SL, Cohen HJ, Hilf R: Evidence against the production of superoxide by photoirradiation of hematoporphyrin. Photochem Photobiol 40: 441–48, 1984
18. Star WM, Marijnissen HP, van den Berg-Blok AE, Versteeg JA, Franken KA, Reinhold HS: Destruction of rat mammary tumor and normal tissue microcirculation by hematoporphyrin derivative photoradiation observed in vivo in sandwich observation chambers. Cancer Res 46(5): 2532–40, 1986
19. Reed MW, Schuschke DA, Ackermann DM, Harty JI, Wieman TJ, Miller FN: The response of the rat urinary bladder microcirculation to photodynamic therapy. J Urology 142(3): 865–68, 1989
20. Henderson BW, Dougherty TJ, Malone PB: Studies on the mechanism of tumor destruction by photodynamic therapy. In: D.R. Doiron and C.J. Gomer editors. Porphyrin localization and treatment of tumors. New York, Alan R. Liss, p. 601–12, 1984
21. Beck TM, Hart NE, Woodard DA, Smith CE: Local or regionally recurrent carcinoma of the breast: results of therapy in 121 patients. J Clin Oncol 1(6): 400–5, 1983
22. Sperduto PW, DeLaney TF, Thomas G, Smith P, Dachowski LJ, Russo A, Bonner R, Glatstein E: Photodynamic therapy for chest wall recurrence in breast cancer. Int J Rad Onc Bio Phy 21(2): 441–6, 1991
23. Wilson CA, Saloupis P, Hatchell DL: Treatment of experimental preretinal neovascularization using photodynamic thrombosis. Invest. Ophthal & Vis Sci 32(9): 2530–5, 1991
24. Miller JW, Stinson WG, Gregory WA, el-Koumy HA, Puliafito CA: Phthalocyanine photodynamic therapy of experimental iris neovascularization. Ophthalmology 98(11): 1711–9, 1991
25. Leonessa F, Green D, Licht T, Wright A, Wingate-Legette K, Lippman J, Gottesman MM, Clarke R: MDA435/LCC6 and MDA/LCC6MDR1: ascites models of human breast cancer. Brit J Cancer 73: 154–61, 1996
26. Slovak M L, Ho JP, Bhardwaj G, Kurz EU, Deeley RG, Cole SP: Localization of a novel multidrug resistance-associated gene in the HT1080/DR4 and H69AR human tumor cell lines, Cancer Res 53(14): 3221–5, 1993
27. Fry DW, Kraker AJ, Connors RC, Elliott WL, Nelson JM, Showalter HD, Leopold WR: Strategies for the discovery of novel tyrosine kinase inhibitors with anticancer activity. Anti-Cancer Drug Design 9(4): 331–51, 1994
28. Martiny-Baron G, Kazanietz mg, Mischak H, Blumberg PM, Kochs G, Hug H, et al.: Selective inhibition of protein kinase C isoenzymes by the indolocarbazole Go 6976. J Biol Chem 268: 9194–7, 1993
29. Skehan P, Storeng R, Scudiero D, Monks A, McMahon J, Vistica D, Warren JT, Bokesch H, Kenney S, Boyd MR: New Colorimetric Cytotoxicity Assay for Anticancer-Drug Screening. J Natl Can Inst 82(13): 1107–12, 1990
30. Holford NH, Scheiner LB: Understanding the dose-effect relationship: Clinical applications of pharmacokinetic-pharmacodynamic models. J Clin Pharmocokin 6(6): 429–53, 1981
31. Nash JC: Compact Numerical Method for Computers: Linear Algebra and Function Minimisation, New York: John Wiley & Sons, 1979
32. Morales DE, McGowan KA, Grant DS, Maheshwari S, Bhartiya D, Cid MC, Kleinman HK, Schnaper HW: Estrogen promotes angiogenic activity in human umbilical vein endothelial cells in vitro and in a murine model. Circulation 9(3): 755–63, 1995
33. Danesi R, Del Bianchi S, Soldani P, Campagni A, La Rocca RV, Myers CE, Paparelli A, Del Tacca M: Suramin inhibits bFGF-induced endothelial cells proliferation and angiogenesis in the chick chorioallantoic membrane. Brit J Cancer 68: 932–8, 1993
34. Kibbey MC, Grant DS, Kleinman HK: Role of the SIKVAV site of laminin in promotion of angiogenesis and tumor growth: an in vivo matrigel model. J Natl Can Inst 84(21): 16633–8, 1992
35. Sharma A, Pizzolanti G, Oh L, Dougherty TJ, Bernacki RJ: Combination of photodynamic therapy and antiangiogenic therapy for the treatment of human breast cancer in nude athymic mice. Proc Amer Assoc Cancer Res 37: A1980, 1996
36. Henderson BW, Bellnier DA, Greco WR, Sharma A, Pandey RK, Vaughan LA, Weishaupt KR, Dougherty TJ: An in vivo quantitative structure-activity relationship for a congeneric series of pyropheophorbide derivatives as photosensitizers for photodynamic therapy. Cancer Res 57(18): 4000–7, 1997
37. Nicosia RF, Ottinetti A: Modulation of microvascular growth and morphogenesis by reconstituted basement membrane gel in three-dimensional cultures of rat aorta: a comparative study of angiogenesis in matrigel, collagen, fibrin, and plasma clot. In Vitro Cell Dev Bio 26(2): 119–28, 1990
38. Weidner N, Folkman J: Tumoral vascularity as a prognostic factor in cancer. Important Advances in Oncology 167–90, 1996
39. Fidler IJ, Ellis LM. The implications of angiogenesis for the biology and therapy of cancer metastasis. Cell 79(2): 185–88. 1994

40. Shalaby F, Rossant J, Yamaguchi TP, Gertsenstein M, Wu XF, Breitman ML, Schuh AC: Failure of blood-island formation and vasculogenesis in Flk-1-deficient mice. Nature (London) 376: 62–66, 1995
41. Fong G, Rossant J, Gertsenstein M, Breitman ML: Role of the flt-1 receptor tyrosine kinase in regulating the assembly of vascular endothelium. Nature (London) 376: 66–70, 1995
42. Soriano P: Abnormal kidney development and hematological disorders in PDGF β-receptor mutant mice. Genes & Dev 8: 1888–96, 1994
43. Schatteman GC, Motley ST, Effmann EL, Bowen-Pope DF: Platelet-derived growth factor receptor alpha subunit deleted patch mouse exhibits severe cardiovascular dysmorphogenesis. Teratology 51: 351–66, 1995
44. Yamaguchi TP, Harpal K, Henkemeyer M, Rossant J: Fgfr-1 is required for embryonic growth and mesodermal patterning during mouse gastrulation. Genes & Dev 8(24): 3032–44, 1994
45. Brunton VG, Kelland LR, Lear MJ, Montgomery GJ, Robertson JH, Robinson DI, Queen J, Workman P: Synthesis and biological evaluation of a series of tyrphostins containing nitrothiophene moieties as possible epidermal growth factor receptor tyrosine kinase inhibitors. Anti-Cancer Drug Design 11(4): 265–95, 1996
46. Gazit A, Osherov N, Gilon C, Levitzki A: Tyrphostin.6. dimeric benzylidenemalononitrile tyrophostins-potent inhibitors of EGF receptor tyrosine kinase *in vitro*. J Med Chem 39(25): 4905–11, 1996
47. Sawutz DG, Bode DC, Briggs GM, Reid JR, Canniff P, Caldwell L, Faltynek CR, Miller D, Dunn JA, de Garavilla L, Guiles JW, Weigelt C, Michne W, Treasurywala AM, Silver PJ: In vitro characterization of a novel series of platelet-derived growth factor receptor tyrosine kinase inhibitors. Biochem Pharm 51(12): 1631–8, 1996
48. Kohn EC, Liotta LA: Molecular insights into cancer invasion: strategies for prevention and intervention. Cancer Res 55: 1856–62, 1995
49. Eckhardt SG, Pluda JM: Development of angiogenesis inhibitors for cancer therapy. Inv New Drugs 15: 1–3, 1997
50. Voest EE: Inhibitors of angiogenesis in a clinical perspective, Anti-Cancer Drugs 7: 723–7, 1996
51. Sharma A, Bernacki RJ: Ovarian cancer patients with CA-125 but no symptoms – Should antiangiogenic treatments be considered? Oncology Res 9(2): 53–4, 1997
52. Dimitroff CJ, Sharma A, Bernacki RJ: Cancer metastasis: a search for therapeutic inhibition. Cancer Invest 16(4): 279–90, 1998
53. Boehm T, Folkman J, Browder T, O'Reilly MS: Antiangiogenic therapy of experimental cancer does not induce acquired drug resistance, Nature 390(27): 404–7, 1997
54. Chang SC, Bown SG: Photodynamic therapy – applications in bladder cancer and other malignancies. J Form Med Assoc 96(11): 853–63, 1997
55. Schuh M, Nseyo UO, Potter WR, Dao T, Dougherty TJ: Photodynamic therapy for palliation of locally recurrent breast carcinoma. J Clin Onc 5(11): 1766–70, 1987
56. Khan SA, Dougherty TJ, Mang TS: An evaluation of photodynamic therapy in the management of cutaneous metastasis of breast cancer. Eur J Cancer 29A: 1686–90, 1993
57. Wilson BD, Mang TS, Stoll H, Jones C, Cooper M, Dougherty TJ: Photodynamic therapy for the treatment of basal cell carcinoma. Arch Derm 128(12): 1597–601, 1992
58. Narayan S, Sivak MV. Jr: Palliation of esophageal carcinoma. Laser and photodynamic therapy. Chest Surg Clin North Amer 4(2): 347–67, 1994
59. Nseyo UO, Dougherty TJ, Boyle DG, Potter WR, Wolf R, Huben R, Pontes JE: Whole bladder photodynamic therapy for transitional cell carcinoma of the bladder, Urology 26(3): 274–80, 1985
60. Dougherty TJ: Photodynamic therapy: status and potential. Oncology 3(7): 67–73, 1989
61. Dougherty TJ: Photodynamic therapy for early stage lung cancer. Preferable to resection? Chest 102(5): 1319–22, 1992

Address for offprints: Ralph J. Bernacki, Roswell Park Cancer Institute, Grace Cancer Drug Center, Department of Pharmacology and Therapeutics, Buffalo, NY 14263, USA; Tel.: (716)-845-3058; Fax: (716)-845-8857; E-mail: bernacki@sc2103.med.buffalo.edu

Phthalocyanine Photodynamic Therapy of Experimental Iris Neovascularization

JOAN W. MILLER, MD, WILLIAM G. STINSON, MD, WILLIAM A. GREGORY, PhD, HAMDY A. EL-KOUMY, MD, CARMEN A. PULIAFITO, MD

Abstract: Photodynamic therapy using chloroaluminum sulfonated phthalocyanine (CASPc) effectively closed experimental iris neovascularization induced in 6 eyes of cynomolgus monkeys by argon laser retinal vein occlusion. Neovascularization was followed by iris photography, fluorescein angiography, and histopathologic examination by light and electron microscopy. Intravenous injection of CASPc followed by irradiation with 675 nm light damaged endothelial cells and pericytes, leading to exposure of the basal lamina and thrombotic occlusion of the blood vessels. Surrounding tissue appeared preserved without evidence of thermal damage. Resorption of occluded vessels by macrophages began 2 to 3 days after photodynamic therapy. Neovascularization reappeared 7 days after photodynamic therapy, probably representing growth of new vessels. Photodynamic therapy with CASPc may be a useful adjunct in the treatment of iris neovascularization. The model is useful in elucidating the ultrastructural changes observed after photodynamic therapy using phthalocyanines. *Ophthalmology 1991; 98:1711–1719*

Iris neovascularization is a serious complication of ocular ischemia. It is associated with many ocular disorders including central vein occlusion, diabetic retinopathy, choroidal melanoma, carotid occlusive disease, and long-standing retinal detachment.[1] The pathogenesis of iris neovascularization remains unclear but is believed to involve the release of factors from ischemic retina or tumors, which stimulate new vessel growth in the iris.[2,3] Iris neovascularization is currently treated by panretinal photocoagulation or peripheral retinal cryopexy, which may act by altering the balance of angiogenic stimulators and inhibitors.[4] Retinal ablation eventually causes regression of iris vessels in 80% of eyes with rubeosis.[5,6] However, in some cases, neovascularization of the angle may progress to angle closure and intractable glaucoma before retinal ablation can take effect.[7] Simmons et al[7] proposed a technique of argon laser goniophotocoagulation to close new iris vessels thermally and stabilize the angle until retinal ablation takes effect. Goniophotocoagulation requires precise application of laser to individual vessels, necessitating a clear view of the angle and a cooperative patient. A better therapy for iris neovascularization would allow selective closure of iris vessels through hazy media, without damage to surrounding tissue. Photodynamic therapy has these theoretical advantages.

Photodynamic therapy is a developing treatment modality that relies on photochemical effects produced in photosensitized tissues exposed to low-intensity light. A photosensitizing dye is injected intravenously, and the targeted tissue is then irradiated at the absorbance maximum of the dye. The activated dye in its triplet state interacts with oxygen and other compounds to form reactive intermediates such as singlet oxygen, which can

Originally received: April 3, 1991.
Revision accepted: May 23, 1991.

From the Laser Research Laboratory, Massachusetts Eye and Ear Infirmary, and the Department of Ophthalmology, Harvard Medical School, Boston.

Presented in part as a poster at the Association for Research in Vision and Ophthalmology Annual Meeting, Sarasota, 1990.

Supported in part by NIH 5 RO1 GM 35459-05 and ONR Contract NOOO14-86-K-0117.

The authors certify that they have no affiliation with or financial interest in the subject matter or materials discussed in the manuscript.

Reprint requests to Joan W. Miller, MD, Retina Service, Massachusetts Eye and Ear Infirmary, 243 Charles St, Boston, MA 02114.

then cause disruption of cellular structures.[8-10] Cellular targets that have been proposed as the site of action include the cell membrane, mitochondria, lysosomes, and the nucleus.[11,12] The photosensitizing dyes are preferentially retained in tumors and neovascular tissue, which can then be selectively targeted.[9,13]

Photodynamic therapy has been demonstrated to cause photoinactivation of cell lines in vitro.[10,12,14,15] It also has been shown to be effective in vivo against a variety of transplantable tumors, including ocular Greene melanoma,[16] fibrosarcoma, reticulum cell sarcoma, and colorectal carcinoma.[13] These studies have been extended into clinical trials, where photodynamic therapy has been used to treat patients with malignant melanoma, squamous cell carcinoma, bladder transitional cell carcinoma, esophageal carcinoma, and gynecological malignancies.[9,17]

Tumor studies have suggested two mechanisms for the photodynamic therapy effect: a direct cytotoxic effect on tumor cells and vascular occlusion within the tumor.[11,16,18-20] The observation that photodynamic therapy induces vascular occlusion has led investigators to use it to close vessels in non-neoplastic diseases. Rose bengal has been used as a photosensitizer to occlude preretinal vessels in the healthy rabbit[21] and to occlude experimental corneal neovascularization.[22] Packer et al[23] used hematoporphyrin derivative to close experimental iris neovascularization. Kliman et al used phthalocyanines to effectively close choroidal neovascularization in a nonhuman primate model (unpublished data).

Most studies in vivo, and treatment studies in patients have used hematoporphyrin derivative as the photosensitizer. However, it is not an ideal photosensitizer for many reasons. Hematoporphyrin derivative is not a pure compound but a mixture of porphyrins. The porphyrins absorb poorly at longer wavelengths (beyond 600 nm) where penetration through tissue, pigment, and blood is optimal. Hematoporphyrin derivative is retained in skin and results in cutaneous photosensitization for several weeks after its administration.[8,10]

We selected chloroaluminum sulfonated phthalocyanine (CASPc) as the photosensitizer. CASPc is a relatively pure compound that is chemically stable at room temperature and absorbs strongly at 675 nm, a wavelength with excellent tissue penetration. It is an effective and efficient photosensitizer, demonstrated in vitro,[10,14,15] in vivo in tumor models,[13,16,20,24] and in models of neovascularization (Kliman, unpublished data). CASPc is retained by skin, but this does not appear to result in cutaneous photosensitization in animals. It also is retained by healthy liver and spleen[13] without any apparent deleterious effects, but the long-term effects of the dye have not been studied.

Plasma levels of CASPc peak at 6 minutes after intravenous injection in mice and rats.[13,24] Maximum tumor concentration of CASPc occurs 24 to 48 hours after injection, although this varies in different tumors.[13,24] We chose to treat 5 minutes after injection of dye, based on previous investigations of CASPc photodynamic therapy of choroidal neovascularization (Kliman, unpublished data).

MATERIALS AND METHODS

ANIMALS

Animals were used in accordance with the ARVO resolution on the use of animals in research. Cynomolgus monkeys (weighing 2 to 3 kg) were anesthetized with an intramuscular injection of ketamine hydrochloride (20 mg/kg), diazepam (1.0 mg/kg), and atropine (0.125 mg/kg). Supplemental anesthesia of 5 to 6 mg/kg of ketamine hydrochloride was given as needed. Proparacaine (0.5%) was used for topical anesthesia. Retrobulbar anesthesia (0.5 ml of 2% Xylocaine [Astra, Westborough, MA]) was given for laser treatments. Pupils were dilated as needed with 2.5% phenylephrine and 0.8% tropicamide. Animals were sacrificed with intravenous injection of 0.5 ml of Euthanasia Solution (embutramide 200 mg/ml, mezebonium iodide 50 mg/ml, tetracaine hydrochloride 5 mg/ml; Hoechst Roussel, Somerville, NJ).

PHOTOGRAPHY

Fundus photography and fluorescein angiography were performed with a Canon Fundus CF-60ZA camera (Lake Success, Long Island, NY). For iris photography and fluorescein angiography, an adapter was mounted on the fundus camera containing an achromatic lens with a focal length of 25.4 mm (Newport PACO22) after D'Anna et al.[25] Angiography was performed with 0.1 ml/kg body weight of 10% sodium fluorescein via saphenous vein injection.

HISTOLOGY

All eyes were enucleated under deep anesthesia and fixed overnight in 2.5% glutaraldehyde/2% paraformaldehyde in 0.1 M cacodylate buffer, pH 7.2 at 4° C. For light microscopy, tissue samples were dehydrated and embedded in JB-4 plastic (Polysciences Inc, Warrington, PA) and serially sectioned at 2 microns. The sections were stained with Stevenol's blue stain, and examined with the Olympus BH-2 photomicroscope. For electron microscopy, tissue samples were postfixed in osmium tetroxide and embedded in Quetol (Polysciences Inc., Warrington PA). Sections were stained with uranyl acetate and lead citrate and examined with the Philips #CM 10 transmission electron microscope (Eindhoven, The Netherlands).

PHOTOSENSITIZER

Chloroaluminum sulfonated phthalocyanine (CIBA-Geigy, Greensboro, NC) with an average of three sulfonate groups per molecule was used as a photosensitizer.[24] It was diluted with 0.9% saline and injected via the saphenous vein at 0.5 to 1.0 mg/kg body weight.

LASER DELIVERY SYSTEM

Laser light at 675 nm from a continuous-wave argon-pumped dye laser (Spectra-Physics Model 375B, Balti-

Region

1
2
3
4
5‡
6

* Dye dose is
† Light dose
‡ The treatme
(see text).

Region

7
8
9
10

* Dye dose is
† Light dose

more, MD)
and collimat
the iris could
Power was ve
tech 362, Bo

INDUCTION
NEOVASCUI

All branch
photocoagul
reh model.[26]
avoiding ne
mented by f
raphy.

Slit-lamp
tography an
every 2 to 5
cularization
at the pupilla
showed hype
by leakage o

Table 1. CASPc Photodynamic Therapy

Region	Dye Dose*	Light Dose†	Location	Angiography	Histopathology
1	0.5	34	Nasal half	1 hr: closed	1 hr: 90% closed
2	0.5	34	Whole iris	1 hr: closed 2 days: closed	2 days: 75% closed with resorption of occluded vessels
3	1.0	102	Nasal half	1 hr: closed 3 days: closed	3 days: 75% closed with resorption of occluded vessels
4	1.0	102	Temporal half	1 hr: closed 2 days: closed 5 days: closed	5 days: 75% closed with remnants of occluded vessels
5‡	0.5	68	Temporal half	1 hr: closed 7 days: few vessels 13 days: open, leaking	13 days: open with possible remnants of occluded vessels
6	0.5	34	Nasal half	1 hr: patchy effect 2 days: open 22 days: open	22 days: open

* Dye dose is mg/kg.
† Light dose is Joules/cm².
‡ The treatment parameters for Region 5 are given for the second treatment. The first treatment given 7 days earlier had a patchy, transient effect (see text).

Table 2. CASPc Photodynamic Therapy

Region	Dye Dose*	Light Dose†	Location	Angiography	Histopathology
7	N/A	34	Temporal half	1 hr: open	1 hr: typical neovascularization
8	N/A	68	Nasal half	1 hr: open 5 days: open	5 days: typical neovascularization
9	0.5	N/A	Whole iris	1 hr: open 22 days: open	22 days: typical neovascularization
10	1.0	N/A	Temporal half	1 hr: open 3 days: open	3 days: typical neovascularization

* Dye dose is mg/kg.
† Light dose is Joules/cm².

more, MD) was delivered along a 300-μm optical fiber and collimated to a 10-mm diameter beam. Sectors of the iris could be shielded using a hemicircular aperture. Power was verified at the cornea by a power meter (Scientech 362, Boulder, CO).

INDUCTION OF EXPERIMENTAL IRIS NEOVASCULARIZATION

All branch retinal veins were occluded by argon green photocoagulation in a modification of the Virdi and Hayreh model.[26] Veins were occluded near the optic nerve, avoiding nearby arterioles. Vein occlusion was documented by fundus photography and fluorescein angiography.

Slit-lamp examination, pneumotonometry, iris photography and fluorescein angiography were performed every 2 to 5 days after retinal vein occlusion. Iris neovascularization was characterized by dilated, tortuous vessels at the pupillary border and in the midperipheral iris, which showed hyperfluorescence early in the angiogram followed by leakage of fluorescein in the later frames.

CASPc PHOTODYNAMIC THERAPY

Whole irides were treated for 360°, or treated as separate halves using the hemicircular aperture described above. A summary of CASPc photodynamic therapy treatment is given in Table 1. Six iris regions, one of which was a whole iris, were treated with CASPc photodynamic therapy. After injection of 0.5 or 1.0 mg/kg of CASPc, the iris regions were irradiated with 675 nm light, at 200 mW with a 10-mm spot size for 133 to 399 seconds. The light doses used were 34, 68, and 102 J/cm². Table 2 gives the parameters for the CASPc photodynamic therapy controls. Two areas were irradiated with 675 nm of light before CASPc injection as light only controls, with light doses of 34 J/cm² and 68 J/cm². Two other areas, one of which was a whole iris, received CASPc without irradiation.

Slit-lamp examination, pneumotonometry, and iris photography and angiography were performed after 1 hour, and, depending on the animal, at 48 hours, 72 hours, 5 days, 7 days, and 13 days after photodynamic therapy. Animals were enucleated and killed at 1 hour, 48 hours,

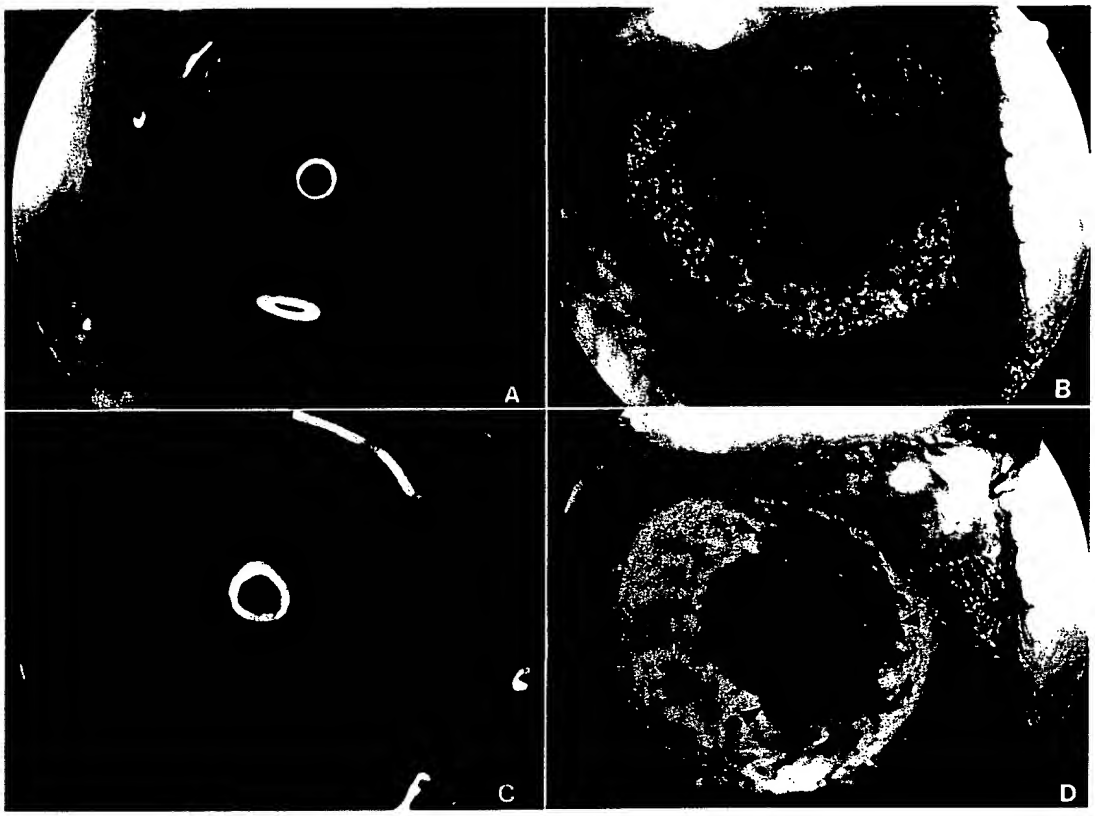

Fig 1. A, iris photograph before treatment with prominent neovascularization over the surface of the iris. B, iris fluorescein angiogram prior to treatment demonstrates fine, tortuous new vessels in the iris, which leaked fluorescein profusely in the later frames. C, iris photograph 1 hour after treatment to the temporal half of the iris (right side of the photo). The arrow indicates a small intrastromal hemorrhage noted after photodynamic therapy. D, iris fluorescein angiogram 1 hour after treatment to the temporal half of the iris. No filling of iris vessels is noted in the treated region (arrowheads). Leakage from iris vessels in the untreated half is already apparent.

72 hours, 5 days, and 13 days after photodynamic therapy, and tissue was processed for histopathologic examination.

RESULTS

VESSEL OCCLUSION

Figure 1 demonstrates the pretreatment and 1 hour post-treatment iris photos and iris angiograms. New vessels were apparent over the surface of the iris before treatment (Fig 1A), and leaked profusely on iris fluorescein angiography (Fig 1B). One hour after photodynamic therapy to the temporal half (right side of the picture), small intrastromal hemorrhages were apparent (Fig 1C), and on iris angiography there was no filling of iris vessels in the treated area (Fig 1D). The hypofluorescence persisted through the angiogram, until it was obscured by leakage from the untreated nasal half of the iris.

Light microscopy (Fig 2) performed 1 hour after photodynamic therapy showed a fibrovascular membrane over the surface of the iris, as well as abnormal, branching vessels deeper in the stroma. Approximately 90% of the vessels were occluded by thrombus, with aggregated platelets and trapped red cells evident. The vascular endothelium was swollen. The stroma and pigment epithelium were apparently unchanged.

Electron microscopy performed 1 hour after photodynamic therapy showed ultrastructural changes in the endothelium of occluded vessels, and in vessels that remained patent. In the affected but patent vessels, the endothelial cells and pericytes demonstrated nuclear swelling and vacuolization of their cytoplasm (Fig 3). In some vessels, areas of attenuated endothelial cell cytoplasm were noted where cytoplasmic processes contacted without apparent junctions (Fig 4). This may represent a change preceding a break in the endothelium. With more severe injury but without vessel occlusion, breaks were apparent in the endothelial cells, with exposure of the basal lamina and adherence of platelets (Fig 4).

Similar damage to the endothelium was observed in occluded vessels (Fig 5). Endothelial cells and pericytes

Fig 2. Light micr
new vessels are ob
iris in a fibrovasc
the vessels are occ
thelium (PE) appe

Fig 3. Electron m
endothelial dama
and vacuolization
cells (E) and peric
(original magnific

demonstrated
adherent to th
lium was disr
dent. The ve
platelets and t
lagen fibers ac
normal striati
in the stroma
areas, pigmen

VESSEL RES

Figure 6 sh
before treatm
the whole iris
after photody

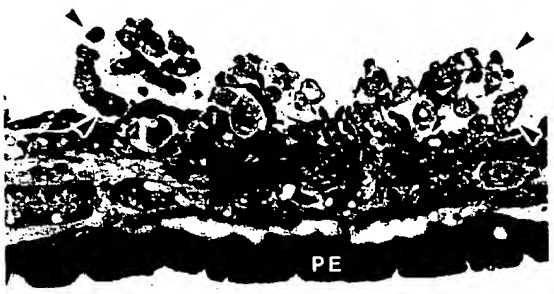

Fig 2. Light micrograph of the iris 1 hour after treatment. Abnormal new vessels are observed in the iris stroma and over the surface of the iris in a fibrovascular membrane (enclosed by arrowheads). Nearly all the vessels are occluded (*). The surrounding stroma and pigment epithelium (PE) appear normal (original magnification, ×200).

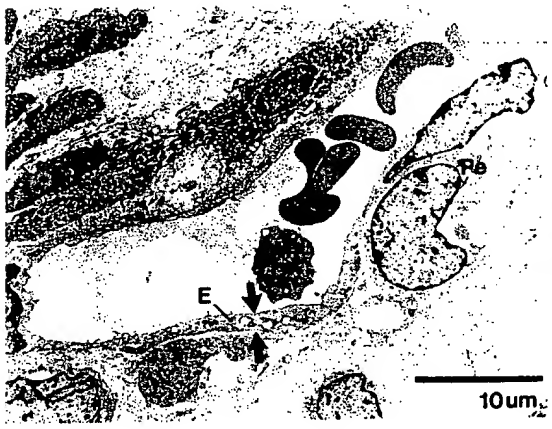

Fig 3. Electron micrograph of iris 1 hour after treatment demonstrating endothelial damage in a patent vessel. There is swelling of the nuclei and vacuolization of the cytoplasm (between arrows) of both endothelial cells (E) and pericytes (Pe). Cells adjacent to the vessel appear undamaged (original magnification, ×1900).

Fig 4. Electron micrograph of iris 1 hour after treatment. A break in the endothelium is evident (between arrows), with exposure of the basal lamina (BL). A platelet (Pl) contacts the basal lamina at this site. The circled region demonstrates two attenuated endothelial cell processes. This change may precede a frank discontinuity in the endothelium with exposure of the basal lamina. C = collagen; Pe = pericyte (original magnification, ×4900).

Fig 5. Electron micrograph of iris 1 hour after treatment. The capillary is occluded with erythrocytes (Er) and platelets (Pl). Platelets are adherent to the basal lamina (BL) in areas of breaks in the endothelium (open arrows). Dense granules (G) released from platelets are evident. The pericyte (Pe) demonstrates a swollen nucleus and vacuolized cytoplasm. Collagen fibers adjacent to the affected vessel demonstrate normal striations and spacing (C–circle) (original magnification, ×4900).

demonstrated pathologic vacuolization. Platelets were adherent to the exposed basal lamina where the endothelium was disrupted. Degranulation of platelets was evident. The vessel lumens were occluded by aggregated platelets and trapped erythrocytes and granulocytes. Collagen fibers adjacent to the affected vessels demonstrated normal striations and spacing (Fig 5). Neighboring cells in the stroma appeared unchanged, although, in some areas, pigment degranulation of stromal cells was noted.

VESSEL RESORPTION

Figure 6 shows iris photos and iris angiograms taken before treatment and 2 days after treatment. In this eye, the whole iris was treated, and the fluorescein angiograms after photodynamic therapy demonstrated a lack of filling of iris vessels (Fig 6D). Fluorescence of limbal vessels confirmed the dye transit. Results of histopathologic examination showed approximately 75% of the vessels to be occluded, with an appearance similar to the changes seen after 1 hour (Fig 7). Collections of packed erythrocytes surrounded by disintegrated endothelium were noted, consistent with partially resorbed, occluded vessels. A few small patent vessels were observed, and in some of these vessels, the endothelial cell nuclei appeared abnormally rounded, protruding into the vessel lumen (Fig 7). This histologic finding is characteristic of iris neovascularization in our experience.

Electron microscopy of iris vessels performed 3 days after treatment showed packed erythrocytes in a vessel

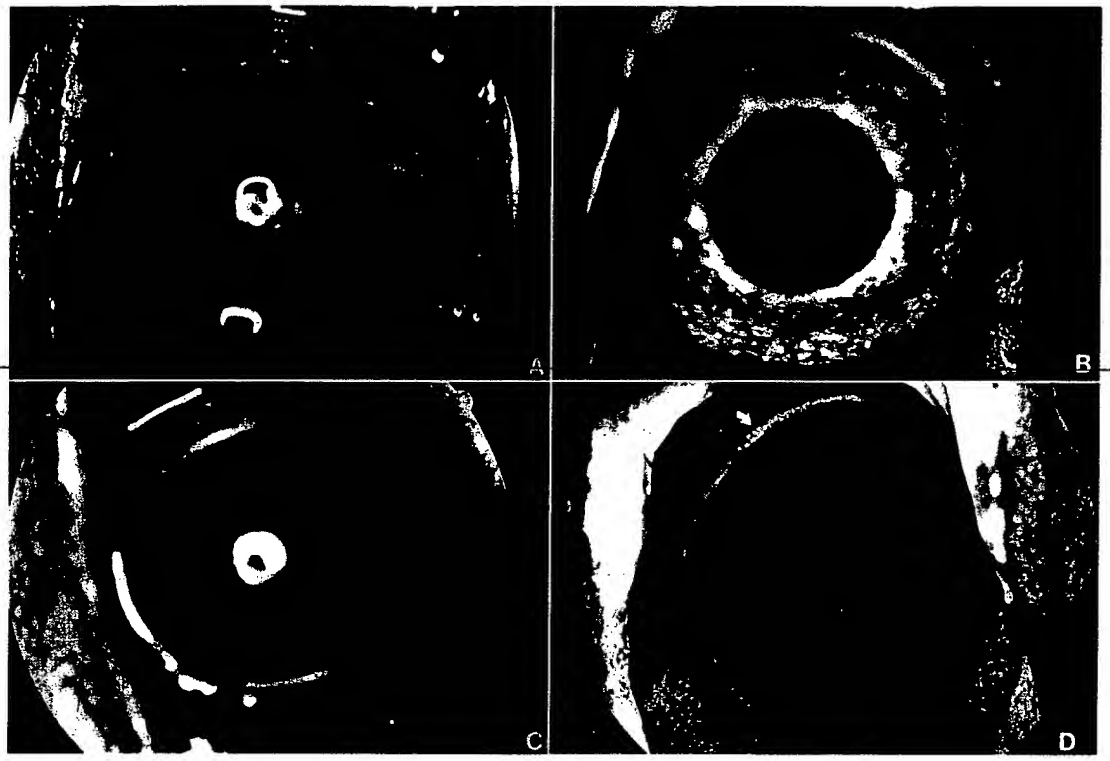

Fig 6. A, iris photograph before treatment. New vessels are noted over the surface of the iris. B, iris fluorescein angiogram before treatment demonstrates fine, tortuous new vessels in the iris, which leaked fluorescein. C, iris photograph 2 days after treatment to the whole iris. Small intrastromal hemorrhages are evident (arrow). D, iris fluorescein angiogram 2 days after treatment. There is no filling of any iris vessels by fluorescein. Fluorescence of limbal vessels confirms the dye transit (arrow).

Fig 7. Light micrograph of iris 2 days after treatment demonstrating occluded vessels on the iris surface and in the stroma (open arrows). In a patent vessel, the endothelial cell nuclei appear abnormally round, protruding into the lumen (arrowhead), a histologic finding characteristic of iris neovascularization (original magnification, ×200).

cast, with only fragments of endothelial cell and pericyte cytoplasm present (Fig 8). Macrophages were observed wrapped around the occluded vessels apparently phagocytosing the endothelium (Fig 9). The basal lamina appeared relatively preserved in areas where the endothelial cells and pericytes were absent.

Five days after treatment, results of electron microscopy showed vessel remnants only (Fig 10). Basal lamina outlined empty lumens, without erythrocytes, endothelial cells, or pericytes. Macrophage processes were noted in proximity to these vessel remnants.

VESSEL RECURRENCE

One region was followed for 13 days after photodynamic therapy. Vessels were angiographically closed for 7 days, when angiographic signs of neovascularization recurred. By 13 days after treatment, the region demonstrated leaking vessels angiographically, with an appearance similar to its pretreatment angiogram. Results of histopathologic examination showed open vessels, both on the surface of the iris and in the stroma (Fig 11). Rare whorls of fibroblast-like cells in the anterior stroma were noted, which were consistent with the remnants of occluded vessels. The stroma appeared undamaged.

LIGHT AND DYE DOSE

Three regions did not demonstrate vessel closure at the light dose initially selected. Regions 5 and 6 (temporal

Fig 8. Electron m
rocytes (Er) are
lamina (BL) is re
heads) are wrapp
magnification, ×

Fig 9. Electron n
(M) is seen phag
lamina (original

and nasal ha
J/cm^2 after t
showed an e
hour after tre
after treatme
ment angiog
treated 9 day
ing the same
of 68 J/cm^2.
as described
topathologic
therapy show
was initially
mg/kg CASI
graphically a
later, again w

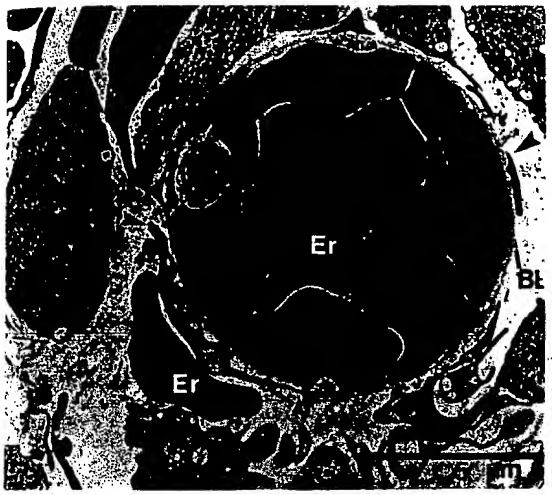

Fig 8. Electron micrograph of iris 3 days after treatment. Packed erythrocytes (Er) are surrounded by disintegrating endothelium. The basal lamina (BL) is relatively well preserved. Macrophage processes (arrowheads) are wrapped around the basal lamina. M = macrophage (original magnification, ×5200).

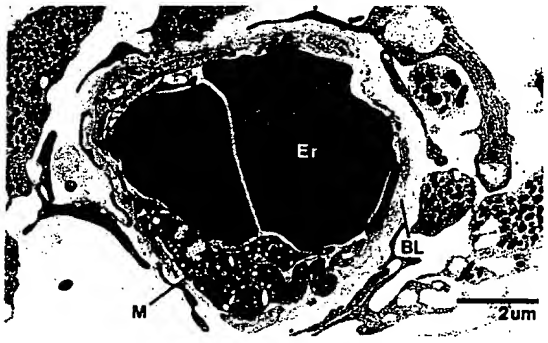

Fig 9. Electron micrograph of iris 3 days after treatment. A macrophage (M) is seen phagocytosing the endothelium. E = erythrocyte; BL = basal lamina (original magnification, ×5200).

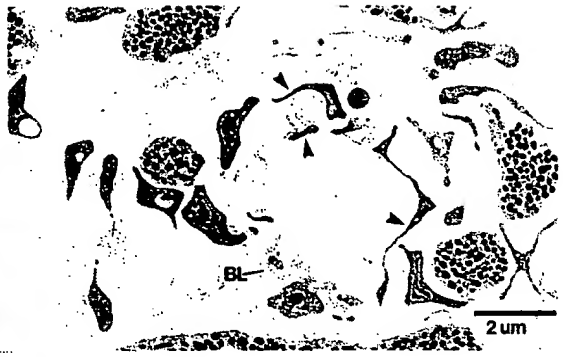

Fig 10. Electron micrograph of iris 5 days after treatment. Basal lamina (BL) outlines an empty lumen, associated with macrophage processes (arrowheads). No endothelial cells or pericytes are seen (original magnification, ×5200).

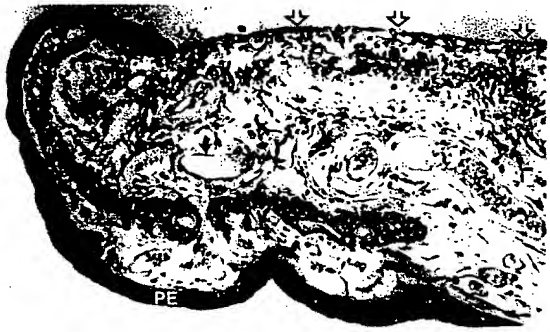

Fig 11. Light micrograph of iris 13 days after treatment. Open vessels are apparent on the surface of the iris and in the stroma (arrows). A fibrovascular membrane is evident over the surface of the iris (open arrows), causing ectropion uveae. PE = pigment epithelium (original magnification, ×100).

and nasal halves of the same iris), were treated at 34 J/cm^2 after the injection of 0.5 mg/kg of CASPc and showed an equivocal patchy closure on angiography 1 hour after treatment. The angiogram performed 48 hours after treatment appeared no different from the pretreatment angiogram. Region 5 (the temporal half) was retreated 9 days after the initial photodynamic therapy, using the same dye dose, but with an increased light dose of 68 J/cm^2. Retreatment successfully closed the vessels as described above. Region 6 was not retreated and histopathologic examination 22 days after the photodynamic therapy showed typical iris neovascularization. Region 4 was initially treated with 68 J/cm^2 after injection of 0.5 mg/kg CASPc, and vessels appeared unchanged angiographically at 1 hour. The treatment was repeated 3 days later, again with no effect. Two days later, the region was treated with 102 J/cm^2 after injection of 1.0 mg/kg CASPc with effective closure of the neovascularization acutely and persistent closure for 5 days as described above.

ADVERSE EFFECTS OF PHOTODYNAMIC THERAPY

Adverse effects of CASPc photodynamic therapy were minimal. An acute rise in intraocular pressure after 1 hour was noted in the treated eyes, ranging from 1 to 23 mmHg (mean, 7.1 mmHg), which resolved within 48 hours. No treatment was given and intraocular pressure measured at follow-up examinations was normal. Mild lid swelling, and chemosis and injection of the conjunctiva were observed, all of which had resolved by 48 hours after treatment. Small intrastromal hemorrhages were noted clinically in two eyes after photodynamic therapy. No hyphemas were observed. Post-treatment inflammation was minimal (in the range of 1+ cell and flare) and transient, resolving by 48 hours after therapy. Although systemic

toxicity was not specifically addressed in this study, no adverse systemic effects of dye administration were noted.

CONTROLS

Control regions irradiated before CASPc injection (Regions 7 and 8), and regions without irradiation but receiving CASPc (Regions 9 and 10), showed no ophthalmoscopic, angiographic, or histologic effect on the neovascularization or the normal stroma.

DISCUSSION

Photodynamic therapy using CASPc effectively closed iris neovascularization in a nonhuman primate model. The ultrastructural changes observed in this model after photodynamic therapy can be combined with what is known biochemically to further elucidate the mechanism of the treatment using phthalocyanines. The model also may be used to investigate the processes of repair and recovery after photodynamic therapy.

The biochemical mechanisms of photodynamic therapy using phthalocyanines and other dyes have been investigated in vitro. The reactions are oxygen dependent and probably involve singlet oxygen.[8,27] Superoxide radicals are formed but their production does not seem to correlate with phototoxicity, and hydroxyl radicals are not generated.[28] Singlet oxygen and other reactive intermediates may oxidatively react with various cellular components including steroids and phospholipids in cell or lysosomal membranes, tryptophan and methionine moieties in proteins, and guanosine moieties in the nuclei.[18]

The cellular effects and subcellular localization of photosensitizing dyes can be demonstrated by ultrastructural studies in vitro. They relate to the biochemical characteristics of a dye and partially determine its photosensitizing efficiency. Porphyrins are hydrophilic compounds and appear to enter the cell by diffusion and localize to the mitochondria.[12] Phthalocyanines are more lipophilic than the porphyrins and have been shown to enter the cell by endocytosis and localize to lysosomes.[12] If endocytosis is inhibited, the phototoxicity of phthalocyanines is greatly reduced but not lost, implying that some phototoxic effect occurs with dye in an extracellular location.

Ultrastructural studies of photodynamic therapy in vivo allow one to observe the mechanism of the treatment in tissue, to elucidate the importance of cell type, vascularity, and surrounding tissue effects. There is increasing evidence that the in vivo mechanism of photodynamic therapy involves vascular damage.[11,18–21] Our findings strongly suggest a selective effect of phthalocyanine photodynamic therapy on blood vessel endothelium. The earliest observed effect of CASPc photodynamic therapy on iris neovascularization was damage to the endothelial cells and pericytes, with nuclear swelling and vacuolization of the cytoplasm. This could be explained by CASPc-mediated photochemical damage to membranes, both extracellular and intracellular (e.g., lysosomes). With increasing photodamage, the endothelial cells appeared to lose their normal junctions and then to retract or "round-up," exposing the basal lamina. Platelets adhered to these areas of exposed basal lamina, and with aggregation and degranulation led to thrombus formation and occlusion of the vessel. Damaged endothelial cells also may contribute to thrombogenesis by the release of Factor VIII as demonstrated by investigators in vitro.[18] Photodamage appeared to be limited to the endothelial cells and pericytes, with nearby stromal cells unaffected. Subendothelial collagen also appeared unaffected with preservation of the typical striations and spacing.

Milanesi et al[20] also found vacuolization and fragmentation of the endothelium 15 hours after photodynamic therapy of transplantable fibrosarcoma, using zinc-phthalocyanine. Packer et al[23] used hematoporphyrin derivative to close experimental iris neovascularization. Histopathology of acutely treated tissue demonstrated empty vessels by light microscopy but changes to individual cells were not described. Barr et al[29] used CASPc photodynamic therapy in normal rat colon and found preservation of collagen with disruption of stromal blood vessels. In contrast, Nelson et al[11] described the earliest effects of CASPc photodynamic therapy in a transplantable mouse tumor as the destruction of collagen fibers in the subendothelial zone with relative preservation of the endothelial cells. Two hours after treatment they observed disruption of blood vessels, and 4 hours after treatment hemorrhage into the tumor obscured histologic details in their model. The tendency for tumors to hemorrhage after photodynamic therapy make them generally less satisfying models for examining the effects of the treatment on microvasculature.

The iris neovascularization model also allows better elucidation of the ultrastructural changes of tissue recovery after photodynamic therapy. Two to three days after the treatment, occluded vessels were observed undergoing resorption. Macrophage processes were wrapped around the occluded vessels phagocytosing the damaged endothelium. This process was more advanced by 5 days after treatment, and, by 13 days after treatment, only rare remnants of occluded vessels were observed in the treated tissue. Frank recanalization of iris vessels was not observed histologically. One region followed for 13 days after photodynamic therapy developed neovascularization angiographically after 7 days, most likely representing recurrence of new vessels secondary to continued angiogenic stimulus from the ischemic retina.

As described in the Results section, three regions did not respond to the initial light and dye doses used. The explanation for a higher light and dye dose requirement is not entirely clear and may relate to the degree of leakage or density of the iris vessels, or differing degrees of pigmentation. However, the dye dose of 1 mg/kg and the light dose of 102 J/cm^2, which were subsequently effective are still low and did not result in any damages to surrounding tissue or systemic toxicity.

In conclusion, CASPc photodynamic therapy effectively closed iris neovascularization, and the vessels remained closed for up to 7 days. Although there was a mild pressure rise after PDT, there were no significant complications of

treatment. Definitive treatment of anterior segment neovascularization requires ablation of retinal tissue, currently best accomplished by panretinal photocoagulation. However, panretinal photocoagulation is not immediately effective, and anterior segment neovascularization can continue to progress in the days to weeks after the treatment. CASPc photodynamic therapy used concurrently with panretinal photocoagulation may be a useful adjunct to this treatment. CASPc photodynamic therapy could be used to close areas of iris neovascularization or with the addition of a gonio lens to close new vessels in the angle. CASPc photodynamic therapy could be a holding therapy used concurrently with panretinal photocoagulation, to close new vessels and stabilize the eye until panretinal photocoagulation is effective in suppressing neovascularization.

ACKNOWLEDGMENTS

The authors thank Wini Reidy, Charles Lin, and John Jacobson for technical assistance.

REFERENCES

1. Gartner S, Henkind P. Neovascularization of the iris (rubeosis iridis). Surv Ophthalmol 1978; 22:291–312.
2. Schulze RR. Rubeosis iridis. Am J Ophthalmol 1967; 63:487–95.
3. Glaser BM, D'Amore PA, Michels RG, et al. The demonstration of angiogenic activity from ocular tissues. Preliminary report. Ophthalmology 1980; 87:440–6.
4. Glaser BM. Extracellular modulating factors and the control of intraocular neovascularization. An overview. Arch Ophthalmol 1988; 106: 603–7.
5. Wand M, Dueker DK, Aiello LM, Grant WM. Effects of panretinal photocoagulation on rubeosis iridis, angle neovascularization, and neovascular glaucoma. Am J Ophthalmol 1978; 86:332–9.
6. Little HL, Rosenthal AR, Dellaporta A, Jacobson DR. The effect of pan-retinal photocoagulation of rubeosis iridis. Am J Ophthalmol 1976; 81:804–9.
7. Simmons RJ, Deppermann SR, Dueker DK. The role of gonio-photocoagulation in neovascularization of the anterior chamber angle. Ophthalmology 1980; 87:79–82.
8. Kreimer-Birnbaum M. Modified porphyrins, chlorins, phthalocyanines, and purpurins: second-generation photosensitizers for photodynamic therapy. Semin Hematol 1989; 26:157–73.
9. Manyak MJ, Russo A, Smith PD, Glatstein E. Photodynamic therapy. J Clin Oncol 1988; 6:380–91.
10. Moan J, Peng Q, Evensen JF, et al. Photosensitizing efficiencies, tumor- and cellular uptake of different photosensitizing drugs relevant for photodynamic therapy of cancer. Photochem Photobiol 1987; 46: 713–21.
11. Nelson JS, Liaw LH, Orenstein A, et al. Mechanism of tumor destruction following photodynamic therapy with hematoporphyrin derivative, chlorin, and phthalocyanine. J Natl Cancer Inst 1988; 80:1599–1605.
12. Roberts WG, Berns MW. In vitro photosensitization I. Cellular uptake and subcellular localization of mono-L-aspartyl chlorin e_6 chloro-aluminum sulfonated phthalocyanine, and photofrin II. Lasers Surg Med 1989; 9:90–101.
13. Chan WS, Marshall JF, Lam GYF, Hart IR. Tissue uptake, distribution, and potency of the photoactivatable dye chloroaluminum sulfonated phthalocyanine in mice bearing transplantable tumors. Cancer Res 1988; 48:3040–4.
14. Ben-Hur E, Rosenthal I. The phthalocyanines: a new class of mammalian cells photosensitizers with a potential for cancer phototherapy. Int J Radiat Biol Relat Stud Phys Chem Med 1985; 47:145–7.
15. Berg K, Bommer JC, Moan J. Evaluation of sulfonated aluminum phthalocyanines for use in photochemotherapy. A study of the relative efficiencies of photoinactivation. Photochem Photobiol 1989; 49:587–94.
16. Panagopoulos JA, Svitra PP, Puliafito CA, Gragoudas ES. Photodynamic therapy for experimental intraocular melanoma using chloroaluminum sulfonated phthalocyanine. Arch Ophthalmol 1989; 107:886–90.
17. Tse DT, Dutton JJ, Weingeist TA, et al. Hematoporphyrin photoradiation therapy for intraocular and orbital malignant melanoma. Arch Ophthalmol 1984; 102:833–8.
18. Zhou CN. Mechanisms of tumor necrosis induced by photodynamic therapy. J Photochem Photobiol [B] 1989; 3:299–318.
19. Wieman TJ, Mang TS, Fingar VH, et al. Effect of photodynamic therapy on blood flow in normal and tumor vessels. Surgery 1988; 104: 512–7.
20. Milanesi C, Biolo R, Reddi E, Jori G. Ultrastructural studies on the mechanism of the photodynamic therapy of tumors. Photochem Photobiol 1987; 46:675–81.
21. Nanda SK, Hatchell DL, Tiedeman JS, et al. A new method for vascular occlusion. Photochemical initiation of thrombosis. Arch Ophthalmol 1987; 105:1121–4.
22. Huang AJW, Watson BD, Hernandez E, Tseng SCG. Photothrombosis of corneal neovascularization by intravenous rose bengal and argon laser irradiation. Arch Ophthalmol 1988; 106:680–5.
23. Packer AJ, Tse DT, Gu X-Q, Hayreh SS. Hematoporphyrin photoradiation therapy for iris neovascularization. A preliminary report. Arch Ophthalmol 1984; 102:1193–7.
24. Tralau CJ, MacRobert AJ, Coleridge-Smith PD, et al. Photodynamic therapy with phthalocyanine sensitisation: quantitative studies in a transplantable rat fibrosarcoma. Br J Cancer 1987; 55:389–95.
25. D'Anna SA, Hochheimer BF, Joondeph HC, Graebner KE. Fluorescein angiography of the heavily pigmented iris and new dyes for iris angiography. Arch Ophthalmol 1983; 101:289–93.
26. Virdi PS, Hayreh SS. Ocular neovascularization with retinal vascular occlusion. I. Association with experimental retinal vein occlusion. Arch Ophthalmol 1982; 100:331–41.
27. Rosenthal I, Murali Krishna C, Riesz P, Ben-Hur E. The role of molecular oxygen in the photodynamic effect of phthalocyanines. Radiat Res 1986; 107:136–42.
28. Ben-Hur E, Carmichael A, Riesz P, Rosenthal I. Photochemical generation of superoxide radical and the cytotoxicity of phthalocyanines. Int J Radiat Biol Relat Stud Phys Chem Med 1985; 48:837–46.
29. Barr H, Tralau CJ, Boulos PB, et al. The contrasting mechanisms of colonic collagen damage between photodynamic therapy and thermal injury. Photochem Photobiol 1987; 46:795–800.